



The Scope of Direct Alkylation of Gold Surface with Solutions of C_1 – C_4 *n*-Alkylstannanes

Eva Kaletová,[†] Anna Kohutová,[†] Jan Hajdúch,[†] Jiří Kaleta,[†] Zdeněk Bastl,[‡] Lubomír Pospíšil,[‡] Ivan Stibor,[†] Thomas F. Magnera,[§] and Josef Michl^{*,†,§}

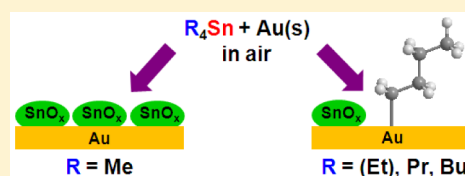
[†]Institute of Organic Chemistry and Biochemistry, Academy of Sciences of the Czech Republic, 16610 Prague 6, Czech Republic

[‡]J. Heyrovský Institute of Physical Chemistry, Academy of Sciences of the Czech Republic, 18223 Prague 8, Czech Republic

[§]Department of Chemistry and Biochemistry, University of Colorado, Boulder, Colorado 80309-0215, United States

S Supporting Information

ABSTRACT: Treatment of cleaned gold surfaces with dilute tetrahydrofuran or chloroform solutions of tetraalkylstannanes (alkyl = methyl, ethyl, *n*-propyl, *n*-butyl) or di-*n*-butylmethylstannyl tosylate under ambient conditions causes a self-limited growth of disordered monolayers consisting of alkyls and tin oxide. Extensive use of deuterium labeling showed that the alkyls originate from the stannane and not from ambient impurities, and that trialkylstannyl groups are absent in the monolayers, contrary to previous proposals. Methyl groups attached to the Sn atom are not transferred to the surface. Ethyl groups are transferred slowly, and propyl and butyl rapidly. In all cases, tin oxide is codeposited in submonolayer amounts. The monolayers were characterized by ellipsometry, contact angle goniometry, polarization modulated IR reflection absorption spectroscopy, X-ray photoelectron spectroscopy, and electrochemical impedance spectroscopy with ferrocyanide/ferricyanide, which revealed a very low charge-transfer resistance. The thermal stability of the monolayers and their resistance to solvents are comparable with those of an *n*-octadecanethiol monolayer. A preliminary examination of the kinetics of monolayer deposition from a THF solution of tetra-*n*-butylstannane revealed an approximately half-order dependence on the bulk solution concentration of the stannane, hinting that more than one alkyl can be transferred from a single stannane molecule. A detailed structure of the attachment of the alkyl groups is not known, and it is proposed that it involves direct single or multiple bonding of one or more C atoms to one or more Au atoms.



INTRODUCTION

The self-limiting formation of alkyl-containing monolayers on metal surfaces by treatment with alkanethiols has been known for over half a century,^{1–6} and has been of much use in recent decades for various applications in nanoscience and nanotechnology.⁷ Such sulfur-mediated attachment of alkyls and other organic moieties to the surface of gold has many advantages, especially easy generation in solution under ambient conditions, and a few disadvantages, such as moderate but distinct sensitivity to oxidation^{8–10} and relatively poor electrical conductivity.^{11,12}

The much more recently discovered^{13,14} self-limiting formation of alkyl-containing monolayers on gold surface by treatment with ambient solutions of alkylstannanes of the types $(C_{18}H_{37})_3SnX$, $(C_{18}H_{37})_2(CH_3)SnX$, and $(C_{18}H_{37})(CH_3)_2SnX$, where the leaving group *X* is triflate, trifluoroacetate, or tosylate, offers an alternative easy access to alkyl-covered gold surfaces. The resulting monolayers do not contain the leaving group *X* and initially we thought that they contain trialkylstannyl groups attached to the gold surface through Sn–Au bonds. It was puzzling that they had the same ellipsometric thickness and other properties regardless of which of the nine stannane precursors was used. Some of these properties are significantly different from those of alkanethiol-based monolayers. In particular, the monolayers

formed from the stannanes are somewhat more resistant to oxidation, and above all, are disordered and block an electrode surface only very weakly. While permeability would be a disadvantage in many applications, it could be an advantage in others that require simultaneous gold surface functionalization and solute access.

In retrospect, the puzzling observation that all nine stannanes examined produced essentially identical monolayers of the same ellipsometric thickness would have been most simply rationalized by postulating that from any one of the reagents one or more long alkyl chains were transferred to the gold surface under formation of C–Au bonds and the rest of the reagent was lost to solution, but this was not proposed. It is the conclusion reached presently, except that we have now discovered that under ambient conditions tin oxide is codeposited on the surface along with the alkyl groups.

The first step toward such a recognition was taken by another group of authors,¹⁵ who measured remarkably high single-molecule conductivities starting with alkane chains terminated with trimethylstannyl groups on each end for attachment to gold electrodes, and proposed that an alkyl-trimethylstannyl bond was cleaved and both residues were

Received: July 22, 2015

Published: September 1, 2015



Table 1. Organostannanes 1–15

$R_1R_2R_3R_4Sn$	R_1	R_2	R_3	R_4
1	CD_3	CD_3	CD_3	CD_3
2	CD_2CD_3	CD_2CD_3	CD_2CD_3	CD_2CD_3
3	$CD_3CH_2CH_2$	$CD_3CH_2CH_2$	$CD_3CH_2CH_2$	$CD_3CH_2CH_2$
4	$CH_3CH_2CH_2$	$CH_3CH_2CH_2$	$CH_3CH_2CH_2$	$CH_3CH_2CH_2$
5	$CD_3CD_2CD_2CD_2$	$CD_3CD_2CD_2CD_2$	$CD_3CD_2CD_2CD_2$	$CD_3CD_2CD_2CD_2$
6	$CH_3CH_2CH_2CH_2$	$CH_3CH_2CH_2CH_2$	$CH_3CH_2CH_2CH_2$	$CH_3CH_2CH_2CH_2$
7	$CH_3CH_2CH_2CH_2$	$CH_3CH_2CH_2CH_2$	$CH_3CH_2CH_2CH_2$	CH_3
8	$CH_3CH_2CH_2CH_2$	$CH_3CH_2CH_2CH_2$	$CH_3CH_2CH_2CH_2$	CD_3
9	$CH_3CH_2CH_2CH_2$	$CH_3CH_2CH_2CH_2$	CH_3	CH_3
10	$CH_3CH_2CH_2CH_2$	$CH_3CH_2CH_2CH_2$	CD_3	CD_3
11	$CH_3CH_2CH_2CH_2$	CH_3	CH_3	CH_3
12	$CH_3CH_2CH_2CH_2$	CD_3	CD_3	CD_3
13	$CD_3CD_2CD_2CD_2$	CH_3	CH_3	CH_3
14	$CD_3CD_2CD_2CD_2$	CD_3	CD_3	CD_3
15	$CH_3CH_2CH_2CH_2$	$CH_3CH_2CH_2CH_2$	CH_3	OTs^a

^aTs = *p*-toluenesulfonyl.

directly attached to the gold surface. Their experiment did not permit other types of measurement, but they provided convincing evidence for C–Au bond formation by comparison with experiments that started with an alkyl chain terminated on each end with phosphine-protected gold atoms. Additional conductivity^{16–18} and mechanistic¹⁹ studies have appeared since and it is now accepted that the attachment to the surface occurs through C–Au bonds. The authors provided no evidence for the presence of trimethylstannyl groups on the gold surface that they proposed, and we shall see below that they are indeed absent. Their mechanism does not account for the formation of identical monolayers from the nine stannanes investigated earlier, but the recognition that C–Au bonds were formed was a critical step forward.

We obtained independent evidence for alkyl attachment to a gold surface through direct C–Au bonding by reaction with a main group organometallic starting with alkylmercury derivatives, with either a long ($n\text{-C}_{18}\text{H}_{37}$)²⁰ and a short (C_4H_9)²¹ chain. This proof was provided by X-ray photoelectron spectroscopic measurements of atomic surface concentrations in the initially produced films and, most convincingly, in films from whose surface mercury was removed, either by electrochemical anodic stripping or simply by heating. Interestingly, our initial experiments with stannanes were motivated by observations of the adhesion of certain organomercurials to gold^{22–24} and, more distantly, the even earlier observations of the adhesion of organoplatinum compounds to platinum surfaces.²⁵

Attachment of organic groups other than alkyls by direct C–Au bonding is also known and can be accomplished, for instance, by treatment with aryldiazonium salts,^{26,27} terminal acetylenes,^{28–30} and carbenes.³¹ Single-molecule junctions obtained by metal–carbon coupling were also reported for fullerene^{32,33} and benzene.³⁴

The purpose of the present paper is to explore the scope of the alkylation of gold surface under ambient conditions with organostannanes carrying short alkyls, methyl to *n*-butyl. We have used a series of stannanes 1–15 (Table 1) carrying either four alkyls or three alkyls and a tosylate leaving group on a tin atom, and characterize the properties of the resulting alkyl monolayers. We use deuteration to differentiate the alkyls transferred from a stannane from contaminants originating in

random impurities, whose signals are otherwise difficult to exclude when working in solution in open air.

The codeposition of tin compounds is a disadvantage if purely alkyl coated surfaces are desired. As is to be reported in detail elsewhere,³⁵ it can be avoided if desired by using solutions of hydrated dibutylditosyloxystannane, which appear to coat gold surfaces with butyl groups only, without depositing detectable amounts of tin. We have already noted above that a metal-free butylated gold surface can also be produced with solutions of *n*-butylmercury tosylate followed by subsequent removal of mercury. However, in view of their toxicity, organomercurials are an unlikely candidate for widespread use. Even tin is a toxic element, but an original attempt to replace it with a lighter congener failed when solutions of numerous long-chain alkylsilanes were found not to deposit monolayers on gold surfaces under ambient conditions.¹³

The direct alkylation of gold surfaces with solutions of organometallics under ambient conditions is still in its infancy and the present finding that methyl is not transferred and ethyl is transferred much more slowly than longer alkyls, and that tin oxide is also deposited, only represents a first step toward establishing the detailed structure of the attachment to the gold surface and the mechanism of its formation. It is possible that the terminal carbon atom is attached to one or more gold atoms of the surface and the alkyl is intact, but it is also conceivable that it has lost one or more of its hydrogen atoms and is attached to the surface in a more complicated mode, e.g., as an alkylidene. In the following text, we use the term alkyl in a loose fashion without implying attachment through a single C–Au bond.

The presentation of the results is organized as follows. We first provide initial evidence from measurements of the contact angle α and the ellipsometric thickness d that after a long enough time (several hours), the same film, except for possible deuteration, is produced from the THF solutions of all the stannanes carrying at least one *n*-butyl, 5–15, whereas a different film is produced from the propyl-carrying stannanes 3 and 4. Yet another film is produced much more slowly from the ethyl-carrying 2. No significant monolayer formation is observed with the methyl-carrying 1.

Second, we examine the kinetics of the observed self-limited growth of ellipsometric thickness of the film produced from 6 in a cursory fashion and note that it is of fractional order in the

bulk stannane concentration. This observation calls for a more detailed future study.

Third, we describe the IR spectra of the films, providing further evidence for their identity and pinpointing which alkyls do and which ones do not transfer to the surface. This definition of the reaction scope is the main topic of the paper. A detailed examination of the IR spectra is planned for the future and should include an investigation of the time dependence of their shape during the deposition, which is especially noticeable for **2**, and an investigation of the spectra obtained with stannanes carrying alkyls partially deuteriated in specific positions.

Fourth, we investigate the elemental composition of the alkylated surfaces by XPS and demonstrate the presence of tin oxide on all stannane-treated gold surfaces, even those treated with **1**, which do not carry alkyls.

Fifth, we measure electrode blocking properties of the films by cyclic voltammetry and electrochemical impedance spectroscopy and determine their charge transfer resistance.

Sixth, we report some observations on the thermal stability of the films.

RESULTS

Growth and Macroscopic Properties of the Monolayers. An initial indication of monolayer formation was provided by a gradual change of ellipsometric thickness d and contact angle α toward reproducible final values after keeping a cleaned gold surface inside a dried THF solution of one of the stannanes **1–15** for periods ranging from a few min to 18 h, followed by thorough rinsing and drying. Chloroform solutions were also used for the stannanes **1**, **2**, **3**, and **12** and produced monolayers with similar d values and IR spectra as those deposited from THF. We have not detected any difference between monolayers deposited using different concentrations of a stannane, as long as sufficient time was provided to reach the long-term limit. Unless specified otherwise, all results described below refer to monolayers deposited from THF solutions.

The evaluation of the ellipsometric thickness d requires a knowledge of the index of refraction. The value 1.47 is ordinarily considered appropriate for alkyl chains,³⁶ but as we shall see below, in our case tin oxide is codeposited with the alkyls and would by itself require a value of 2.0.³⁷ An additional uncertainty exists in that some or all of the tin might be present in the form of tin monoxide or suboxide. Since we shall only use the d values in a relative sense, the exact value of the index of refraction is not critical. Arbitrarily, we have adopted the average of the two indices and have used the value 1.74 in all ellipsometric evaluations except for those films that contain no alkyls, in which case we used 2.0, and the alkanethiol films used for comparison, in which case we used 1.47.

In pure solvent, THF or chloroform, d does not increase within the experimental error over a period of 18 h. In 1×10^{-4} to 1×10^{-3} M THF solutions of the methyl-carrying **1** the changes in α and d upon monolayer deposition were very small and barely outside the experimental error. In 1×10^{-4} M THF solutions of ethyl-carrying **2**, the changes in α and d were very slow. The limiting values were only reached after about 18 h and then remained stable. In 5×10^{-4} M THF solution, they were reached after 4–5 h. In the case of the *n*-propyl-carrying **3** and **4**, and of the *n*-butyl-carrying **5–15**, in 1×10^{-4} M THF solutions, both d and α changed distinctly and rapidly at first and converged after a few hours to limiting values that then

remained stable. These final values were $\alpha_{\infty} = 69^{\circ} \pm 4^{\circ}$ and $d_{\infty} = 1.8 \pm 0.5$ Å for the ethyl containing **2**, $\alpha_{\infty} = 77^{\circ} \pm 4^{\circ}$ and $d_{\infty} = 2.8 \pm 0.3$ Å for the propyl containing **3** and **4**, and $\alpha_{\infty} = 90^{\circ} \pm 3^{\circ}$ and $d_{\infty} = 4.3 \pm 0.8$ Å for the butyl containing **5–15**. For CHCl_3 solutions, the final values of d were determined for **1**, **2**, **3** and **12**, and were found to be the same as for THF solutions. Figure 1 shows the final values of the static contact angle α .

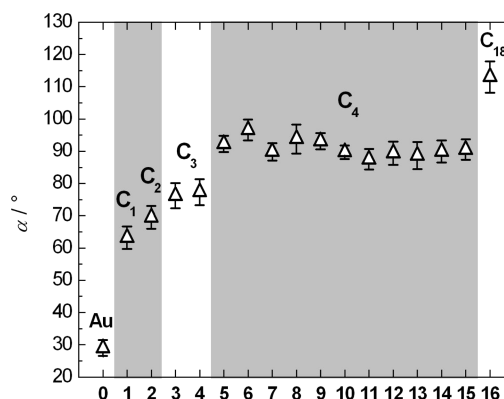
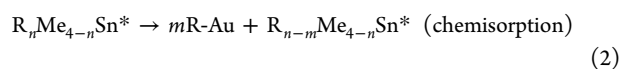
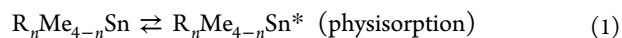


Figure 1. Static contact angle α of water on a cleaned Au substrate (**0**) and its limiting value on films produced after 5 h from 1×10^{-4} M THF solutions of the stannanes **1–15** and from $n\text{-C}_{18}\text{H}_{37}\text{SH}$ (**16**). For the slowly reacting stannane **2**, a 5×10^{-4} M solution was used.

Figure 2A displays the overall time dependence of the thickness d obtained with all of the stannanes. Figure 2B focuses on a selection of six stannanes carrying butyls and methyls and demonstrates that isotopic substitution in either alkyl has a small or no effect on the growth rate within the limits imposed by the experimental accuracy. Although we recognize the limited accuracy of the ellipsometric method for measuring the degree of coverage, we considered it worthwhile to attempt a preliminary global fit of the growth curves of **6** for concentrations ranging from 10^{-5} to 10^{-2} M to a kinetic model, as described next (Figure 3).

Kinetic Model. A reasonable starting point is to assume that the surface reaction of the alkylstannanes follows the well-studied behavior of alkanethiols and dialkyl disulfides^{38–40} and proceeds through two steps, (i) reversible physisorption of the stannane reagent on the gold surface, and (ii) an irreversible surface reaction consisting of a transfer of one or more alkyl groups from the tin atom of the physisorbed stannane to the gold surface. We have taken the $\theta(t,c) = d(t,c)/d_{\infty}$ value as a crude approximation to the fraction of the surface that has been coated at time t in a THF solution containing a constant molar concentration c of a stannane.

We first note that under the reaction conditions the overall process is irreversible in that d_{∞} is independent of c and once produced, the films are not removed by the pure solvent even after a long time. Although an alkylstannane can have as many as four different alkyl groups, we are only dealing with stannanes **1–15** carrying up to two different alkyl groups on the tin atom. Recognizing that most *n*-alkyl groups can be transferred to the surface but methyl cannot, a representation of the standard mechanism is



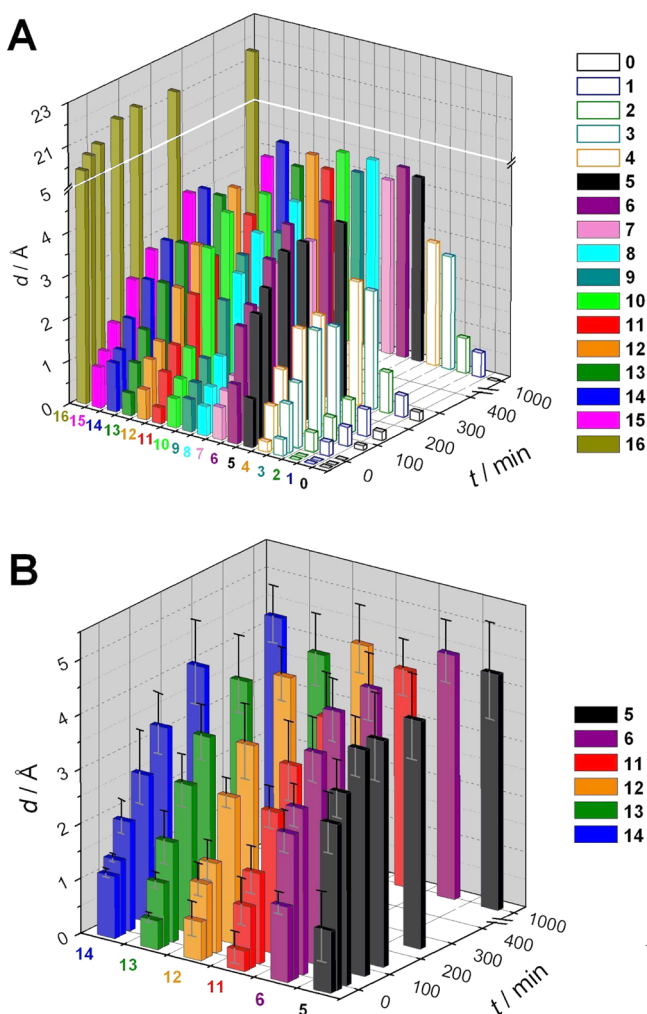


Figure 2. Time dependence of ellipsometric thickness d of a monolayer deposited on a cleaned Au substrate from a 1×10^{-4} M solution in THF. (A) Monolayers of 1–15, compared with n -C₁₈H₃₇SH (16) and pure solvent (0). Estimated precision: ± 0.3 Å for 3 and 4 and ± 0.8 Å for 5–15. (B) Detail: stannanes that differ by deuteration.

where R is an alkyl that can be transferred from tin to the gold surface, and Me is methyl, which cannot be transferred. Reaction 2 may consist of several steps and is followed by (or concurrent with) other transformations of the tin-containing product, such as air oxidation.

We have selected the stannane 6 for a more detailed examination. Fits of the data shown in Figure 3 with models that describe processes in which the film thickness develops through pure diffusion-limited,⁴¹ diffusion-convection-limited,³⁸ and rapid reversible⁴² physisorption were not satisfactory, as they either produced an incorrect temporal dependence of θ or required physisorption/desorption rate constants that were very large and clearly not rate-limiting. Simpler models with fewer fitted parameters were found to be the most statistically meaningful. A regression analysis showed that as the number of parameters increased the curve followed the data better, but the fitted parameters became less self-consistent.

If the surface concentration of available Au sites is $(1 - \theta)$, and if one assumes that the pre-equilibrium shown in step (1) is fast, such that the surface concentration of $R_n\text{Me}_{4-n}\text{Sn}^*$ is proportional to the bulk concentration c , the resulting rate law,

$d\theta(t)/dt = kc^q[1 - \theta(t)]$, integrates to $\theta(t) = 1 - \exp(-kc^qt)$ for simple Langmuir kinetics (q is the order of the surface alkylation reaction in c and equals $1/m$). If the attachment rate is affected by prior coverage, islands, etc.,³⁸ k can be further adjusted by a second $(1 - \theta)$ factor to yield the alternative rate law $d\theta(t)/dt = kc^q[1 - \theta(t)]^2$ (surface-limited Langmuir model). This integrates to $\theta(t) = c^qt/(1 + kc^qt)$.

We have investigated the fits of the data to both rate laws, treating d_∞ for each run as an adjustable parameter and starting with the arbitrarily chosen case $q = 1$ (Figure 3). We then optimized the value of q for the best global fit and found the reaction orders $q = 0.45$ for the simple and $q = 0.46$ for the surface-limited Langmuir model (Figure 3 and Table 2). A first-order dependence on c can be unequivocally ruled out, suggesting that more than one alkyl group is being transferred from a tin atom ($m > 1$), and within the uncertainty in the fit parameters the order is $1/2$. It appears that the surface-limited Langmuir model is somewhat superior to the simple Langmuir model, but it is difficult to decide this with certainty. A decision between these and perhaps other possibilities will clearly require a dedicated kinetic study using a more accurate method of surface coverage assessment than ellipsometry, such as those based on resistivity,³⁸ reflectivity,⁴³ SHG^{44,45} or a quartz microbalance.⁴² This more complete study will also have to use several alkylstannanes with different numbers of transferable alkyl groups n . Such a study lies outside the framework of the present paper, which focuses on establishing the scope of the surface alkylation reaction.

The Alkyls Transferred. The identity of the groups transferred to the gold surface was established by recording the infrared spectra of the monolayers using photomodulation infrared reflection–absorption spectroscopy (PM-IRRAS) with careful background subtraction. The presence of background is hard to avoid when working under ambient conditions and we rely primarily on isotopic labeling of the alkyls present in the stannane to differentiate them from atmospheric impurities. Even though we use polarization modulation to minimize interference by isotropic impurities, some of the background may also be due to C–H vibrations of atmospheric impurities that collect on spectrometer windows and mirrors, if they are partially oriented relative to the surface normal and the light is not incident exactly along the normal.

The assignments of peaks to CH₂, CH₃, CD₂, and CD₃ C–H and C–D stretching vibrations followed the literature.^{46–48} An additional strong peak or shoulder at ~ 2898 cm^{−1} appeared in the ordinary IR spectra of all stannanes 1–15 if and only if they contained an SnCH₂ group and seems to be associated with a perturbed CH₂ vibration in analogy to a similar perturbed CH₂Si antisymmetric stretch vibration of silanes.⁴⁹ Interestingly, an analogous peak is not present in the C–D stretching region, suggesting that it is not due to a fundamental vibration but most likely to a Fermi resonance. However, at the present moment we cannot exclude either possibility with certainty and the association of an intense peak or shoulder at ~ 2898 cm^{−1} with the presence of the SnCH₂ moiety in the molecule is strictly empirical. Only very weak absorptions were observed in the bending region and we were not able to use them for analysis. Weak vibrations in the C=O and C–O stretching regions in the spectra of the films appeared in the crude spectra but were absent within the experimental error after baseline subtraction.

A 3-h immersion in THF-*d*₈ alone, followed by rinsing with THF-*d*₈ and drying, generates weak peaks attributable to CD₂

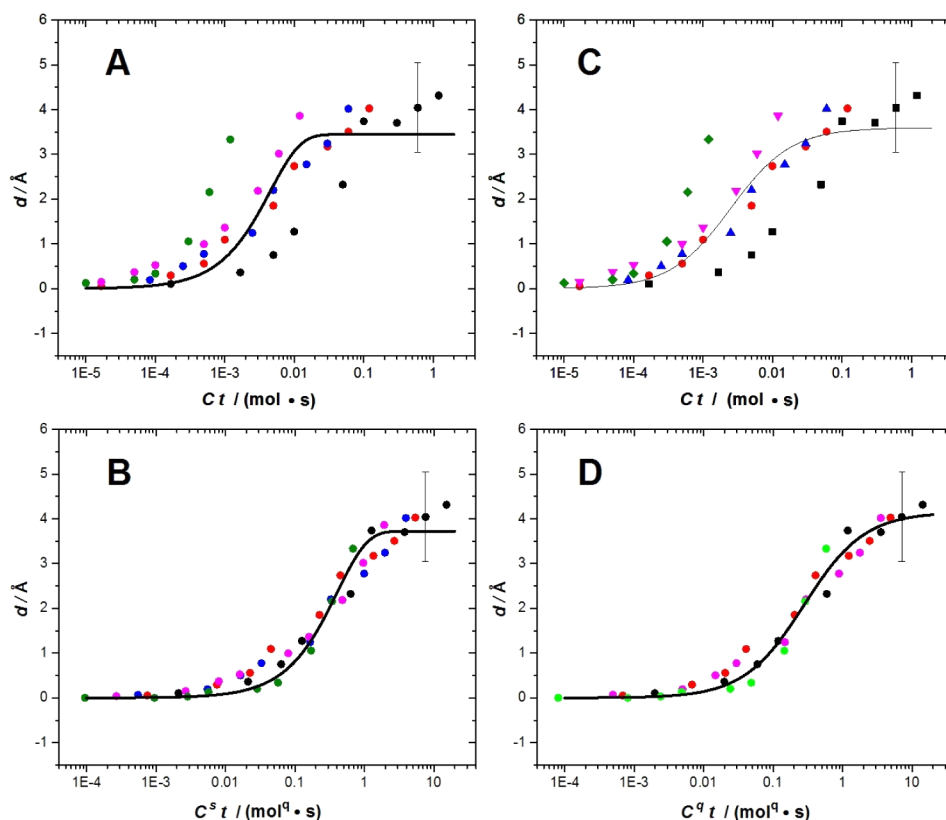


Figure 3. Global fits for concentration-weighted growth curves for compound **6** done for simple Langmuir kinetics (A, B) and surface-limited Langmuir kinetics (C, D) with first-order (A, C) and fit-determined order (B, D) of c . The data are comprised of five separately acquired sets with c : 0.01 M (black), 0.001 M (red), 0.0005 M (blue), 0.0001 M (magenta) and 0.00001 M (green).

Table 2. Fitted Rate Constant and Film Thickness for Gold Surface Alkylation by **6 in a THF Solution**

q^a	simple Langmuir kinetics			surface-limited Langmuir kinetics		
	d_∞ (Å) ^b	k (M ^{-q} s ⁻¹) ^c	q^a	d_∞ (Å) ^b	k (M ^{-q} s ⁻¹) ^c	q^a
1	3.44 ± 0.22	221 ± 52		3.59 ± 0.22	398 ± 1010	
fitted	3.72 ± 0.10	2.47 ± 0.70	0.45 ± 0.03	4.15 ± 0.11	3.60 ± 0.96	0.46 ± 0.03

^aReaction order with respect to bulk stannane concentration c . ^bLimiting film thickness. ^cApparent rate constant, which contains the pre-equilibrium constant from eq 1.

and CD₃ groups, whose origin must be the solvent. The species responsible for these absorptions is or are adsorbed only weakly and subsequent immersion in a THF solution of an undeuterated stannane removes them entirely. These C–D peaks do not form when the gold surface is immersed in a 1×10^{-4} M solution of **6** in THF- d_8 , and only strong signals due to the CH₂ and CH₃ groups derived from **6** are present (Figure S1). Similarly, an initial immersion of the gold surface in THF for a few hours followed by drying does not affect the subsequent deposition of a monolayer from a solution of **2**.

The spectra of gold surfaces treated with 1×10^{-4} M THF or CHCl₃ solutions of **1** for up to 18 h showed no detectable intensity for any C–D stretching vibrations in the 2000 to 2300 cm⁻¹ region. Even at a concentration of 1×10^{-3} M in THF or CHCl₃, no C–D stretching intensity was observed after 18 h. We estimate from the signal-to-noise ratio obtained in the C–D stretching region for the monolayer produced with **3** that a few percent of a monolayer similar to the others would have been detectable for **1**, and conclude that under these conditions methyl groups are not being transferred to the gold surface to any significant extent.

When a gold surface is immersed in a 1×10^{-4} M solution of **2** in THF or CHCl₃ for 5 h, no C–D stretching intensity is observed on the rinsed and dried samples, but after 18 h it appears clearly. When 5×10^{-4} M solutions of **2** in either solvent are used, C–D stretching intensity is obviously present already after 3 h of immersion. We have noted that the spectral shape in the region of the asymmetric CD₃ stretch in these samples changes during extended immersion in the stannane solution in THF and intend to investigate this in detail at a future time.

The spectrum of the monolayer produced from **3** in THF exhibited four main peaks in the CH and CD stretching regions, attributable to CH₂ and CD₃ groups (Figure 4), and leaves no doubt that the propyl group has been transferred to the surface. For comparison, Figure 4 also provides the FTIR-ATR spectrum of pure **3**, and it is apparent that the intensity of the $\nu_s(\text{CD}_3)$ peak relative to the $\nu_{as}(\text{CD}_3)$ peak is enhanced in the spectrum of the monolayer, suggesting that the C–CD₃ bond is inclined toward the surface normal. However, relative integrated intensities do not confirm this trend within experimental error and a reliable conclusion is not possible. No particular alignment is observed for the methylene groups.

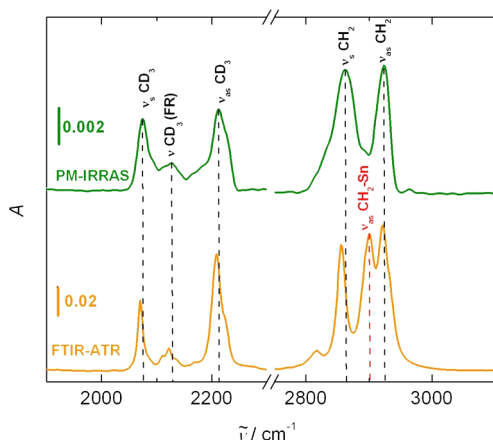


Figure 4. FTIR-ATR spectrum of neat **3** (orange) and PM-IRRAS spectrum of the monolayer produced from **3** on Au substrate (green). FR indicates a Fermi resonance.

The peaks attributable to $\nu(\text{CH}_2\text{-Sn})$ in the spectrum of neat **3** and marked in red in Figure 4 are absent in the spectrum of the monolayer. The IR spectra obtained from **3** in CHCl_3 solution were the same as those obtained from THF solution.

The PM-IRRAS spectra of monolayers obtained from THF solutions of **5**, **6**, and **10** on an Au substrate are displayed in Figure 5 along with the spectra of neat **5** and **6**. The spectra of

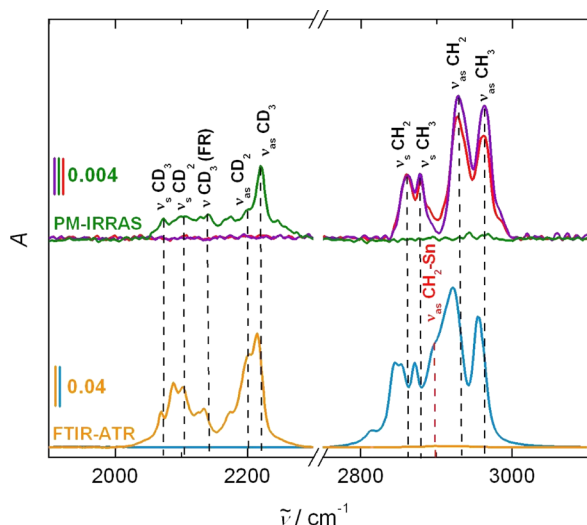


Figure 5. FTIR-ATR spectra of neat **5** (orange) and **6** (blue) and PM-IRRAS spectra of monolayers produced from **5** (green), **6** (violet) and **10** (red) on cleaned Au substrates.

5 and of the monolayer formed from **5** show only vibrations attributable to the CD_3 and CD_2 groups and negligible intensity for CH vibrations that might have arisen from the solvent or from extraneous impurities. The spectra of the monolayers formed from **6** and **10** show CH_3 and CH_2 stretching vibrations. Together, the spectra demonstrate that the butyl groups are transferred to the surface. The absence of CD vibrations in the case of the monolayer produced from **10** reveals that the methyl groups that are also attached to the tin atom of **10** are not transferred to the surface. The CH_2Sn vibrations contribute significantly to the spectrum of neat **6** but not to the spectrum of the monolayer produced from **6** and this is compatible with the notion that the butyl group is transferred

without the tin atom. The differences in relative peak intensities in the spectra of neat compounds and the monolayers are difficult to discern and interpret due to excessive band overlap.

The spectra obtained from THF solutions of **2**, **4**, **7–9**, and **11–15** are provided in Figure S2 and are very similar to those shown here. For **2**, **3** and **12**, a CHCl_3 solution was also used and produced the same IR spectra. In particular, the spectrum of the film obtained from a CHCl_3 solution of **12** contained no C–D stretching intensity, demonstrating that even in this solvent methyl groups are not transferred to the surface. The spectrum of **15** does not contain the peaks expected for the tosyloxy or tosylate groups, such as 3100 cm^{-1} , $\nu(\text{C-H, aromatic})$, 1260 cm^{-1} [$\nu_a(\text{SO}_3^-)$], and 1105 cm^{-1} [$\nu_s(\text{SO}_3^-)$].⁴⁸

The peak frequencies observed for monolayers formed from THF solutions of **1–15** are listed in Table 3. If we assume that isotopic substitution has a negligible effect on the chemical properties of the stannanes (Figure 2B), inspection of the results contained in this table reveals the following: (i) Methyl groups are never transferred from a stannane to the Au surface, and ethyl groups are transferred only very slowly. (ii) *n*-Propyl and *n*-butyl groups are always transferred from a stannane to the Au surface. (iii) The alkyls that have been transferred to the Au surface are no longer attached to tin.

Surface Layer Elemental Composition. X-ray photoelectron spectra (XPS) were recorded for monolayers formed from ten of the stannanes. Under exposure to X-rays in ultrahigh vacuum $\sim 15\%$ of the monolayer can desorb as indicated by a reduction of IR intensity of C–D stretching vibrations of films deposited from THF solutions of **5** and **14** measured before and after the XPS measurement. A mild increase of intensity of C–H vibrations was also noticed, likely originating from contaminating species adsorbed from the ambient during transport of samples. Illustrative spectra are displayed in Figures 6 and 7 and the others are shown in Figures S3 and S4. The measured surface photoemission intensity ratios adjusted by Scofield photoionization cross sections⁵⁰ along with the surface concentration of tin calculated assuming that all of it is located in the very first surface layer and exposed to vacuum are displayed in Table 4.

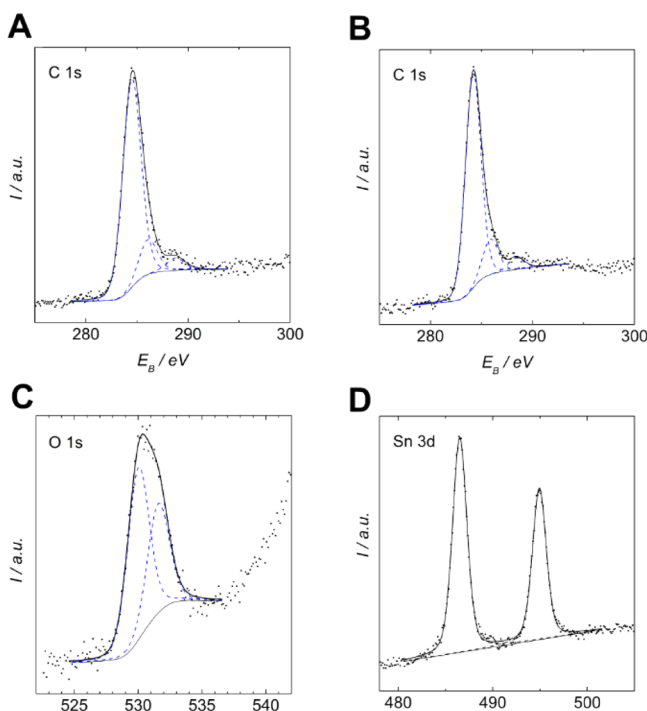
The XPS results revealed the presence of tin in the monolayers prepared from the stannanes. The binding energy obtained for Sn $3d_{5/2}$ photoelectrons, $486.5 \pm 0.1\text{ eV}$, was identical for all samples and was consistent with the presence of tin oxide on the gold surface. This assignment is corroborated by the presence of a component with binding energy of 530.3 eV in the spectra of O $1s$ photoelectrons, which is characteristic of metal oxides,⁵¹ including tin oxide.^{52,53} The Sn $3d_{5/2}$ binding energy shift between Sn^{4+} and Sn^{2+} formal valencies in tin oxides is rather small^{53,54} and thus the measured binding energy does not allow unambiguous differentiation between SnO , SnO_2 or some intermediate stoichiometry. In addition, the available values were measured on bulk oxides and may differ from those for SnO_x nanostructures that can be expected in our samples.

The energy separation between the O $1s$ component belonging to Sn oxide and the Sn $3d_{5/2}$ peak was used by some authors^{54,55} to distinguish between SnO and SnO_2 , even though the difference between the two is small (0.1 eV). Our value, 43.9 eV , fits those reported for SnO_2 . It needs to be noted that the binding energy of Sn $3d_{5/2}$ electrons published⁵⁶ for Bu_4Sn , 486.3 eV , lies within the experimental error of values reported for tin oxides.

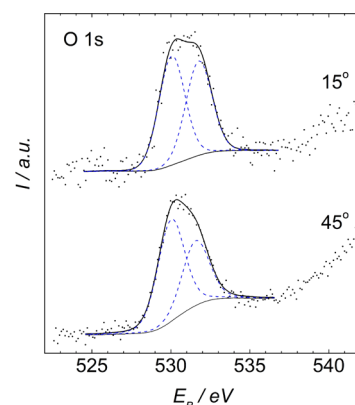
Table 3. CH and CD Stretching Vibrations Observed in the PM-IRRAS of Au Surfaces Treated with THF Solutions of 3–15 (cm^{-1})^a

group	mode	2	3	4	5	6	7	8	9	10	11	12	13	14	15	16
CH ₃	ν_s	—	—	2877	—	2878	2878	2877	2879	2878	2879	2879	×	—	2879	2878
	ν_{as}	—	—	2963	—	2961	2964	2964	2962	2963	2965	2965	×	—	2960	2964
CD ₃	ν_s	2075	2075	—	2074	—	—	×	—	×	—	×	2072	2073	—	—
	ν (FR)	×	2131	—	2132	—	—	×	—	×	—	×	2135	2134	—	—
	ν_{as}	2216	2212	—	2220	—	—	×	—	×	—	×	2220	2219	—	—
CH ₂	ν_s	—	2865	2856	—	2863	2862	2858	2863	2860	2862	2862	—	—	2863	2851
	ν (CH ₂ –Sn)	—	×	×	—	×	×	×	×	×	×	×	—	—	×	—
	ν_{as}	—	2925	2926	—	2928	2930	2929	2929	2925	2929	2929	—	—	2928	2920
CD ₂	ν_s	2186	—	—	2103	—	—	—	—	—	—	—	2103	2102	—	—
	ν_{as}	2149	—	—	2205	—	—	—	—	—	—	—	2206	2203	—	—

^aNo IR peaks were observed for **1**. Significance of symbols: —, this isotope is absent in the stannane used; ×, this isotope is present in the stannane used, but no vibration attributable to it was detected in the spectrum of the monolayer.

**Figure 6.** XPS of layers on Au surface. (A) C 1s, cleaned Au surface immersed for 4 h in pure THF. (B) C 1s, (C) O 1s, and (D), Sn 3d for monolayers formed by treatment of a cleaned gold surface with a 5×10^{-4} M THF solution of **11**.

The spectra of O 1s photoelectrons can be fitted by two components centered at 530.3 and 531.8 eV (see Figure 7 and Figure S4). The former is attributable to tin oxide, and after correction for photoionization cross sections its integrated intensity relative to that of Sn 3d emission yielded an atomic concentration ratio O/Sn = 1.5 ± 0.2 , indicating that SnO, SnO₂ and/or a suboxide might all be present on the Au surface. The high binding energy component of the O 1s peak is due mainly to oxygen in C–O, O=C=O, and –OH groups,⁵⁴ which have similar binding energies and cannot be distinguished. This spectral component is also present in the spectra of gold samples after their immersion in pure THF and subsequent drying, and its intensity depends on the method used for the initial gold surface cleaning. The ratio of intensities of components of the O 1s spectra is different for different samples and is a function of the detection angle of photoelectrons (Figure 7). The relative weight of the higher

**Figure 7.** XPS of O 1s photoelectrons from a cleaned gold surface treated with a 5×10^{-4} M THF solution of **11** measured at two different detection angles (defined from the sample surface).**Table 4.** Sn 3d/Au 4f, C 1s/Au 4f, O 1s/Au 4f, and C 1s/Sn 3d Photoemission Intensity Ratios Adjusted by Scofield Photoionization Cross Sections^a

sample	reagent	Sn/Au	C/Au	O/Au	C/Sn	$c(\text{Sn})^b$
0 ^c	THF	0	0.9	0.28	—	0
1	Sn(CD ₃) ₄	0.04	0.51	0.17	12.8	2.3
2	Sn(C ₂ D ₅) ₄	0.076	0.95	0.41	11.8	4.4
3	Sn(C ₃ H ₄ D ₃) ₄	0.084	0.77	0.31	9.2	4.7
6	Sn(C ₄ H ₉) ₄	0.036	0.55	0.18	15.3	2.3
7	Sn(C ₄ H ₉) ₃ CH ₃	0.087	0.71	0.40	8.2	4.8
8	Sn(C ₄ H ₉) ₃ CD ₃	0.087	0.79	0.46	9.1	4.8
9	Sn(C ₄ H ₉) ₂ (CH ₃) ₂	0.107	0.41	0.16	3.8	6.1
9 ^d	Sn(C ₄ H ₉) ₂ (CH ₃) ₂	0.024	0.26	0.11	10.8	1.4
9 ^e	Sn(C ₄ H ₉) ₂ (CH ₃) ₂	0.18	0.39	0.38	2.2	10.1
10	Sn(C ₄ H ₉) (CD ₃) ₃	0.024	0.53	0.27	22	1.4
11	Sn(C ₄ H ₉) (CH ₃) ₃	0.067	0.53	0.20	7.9	3.9
13	Sn(C ₄ D ₉) (CH ₃) ₃	0.104	0.70	0.27	6.7	5.8
15	SnBu ₂ CH ₂ OTs	0.023	0.46	0.16	20.0	1.3

^aMonolayers formed by treatment of cleaned gold surface with a 5×10^{-4} M solution of a stannane in THF for 4 h. Estimated accuracy, $\pm 10\%$. ^bSurface concentration of tin atoms in units of 10^{14} atoms/cm². The value for a tin monolayer is 11.1. ^cFlame annealed gold film on mica immersed in THF for 4 h without any stannane added.

^dAdsorption from gas phase on template stripped (Platypus) gold substrate. ^eAu surface cleaned by mild Ar⁺ sputtering ($E = 4$ keV, $I = 10$ uA, $t = 10$ min).

binding energy O 1s component increases as the detection angle measured from the sample surface decreases, showing that the responsible oxygen containing functionalities are more distant from the gold surface than the oxygen atoms belonging to tin oxide. This finding indicates that these species are present (adsorbed) on top of the initial monolayer. They likely originate primarily from adventitious contamination or oxidation of samples exposed for certain time to ambient air.

The C 1s spectra revealed that a carbonaceous contamination carrying small amounts of singly and doubly bonded oxygen functionalities is present even on a gold surface immersed in pure THF solvent containing no stannanes, yielding a C/Au ratio close to 1. This carbon species is presumably also responsible for the weak IR intensity in the C–D stretch region when THF- d_8 is used (Figure S1). As noted above, most or all of this species is removed during the process of surface alkylation with a stannane.

For the monolayers prepared from stannane solutions, the C/Au ratio varies from sample to sample within the range 0.2–1. In most instances it is smaller than 1, suggesting that in the presence of a stannane the amount of carbonaceous impurity deposited from the solvent is indeed reduced, and that it does not represent a stable background that could be subtracted. This prevents us from using the C/Au ratio to deduce the surface concentration of the alkyl groups, even if one could correct for the attenuation of the Au signals by an overlayer that contains variable amounts of tin.

The core level binding energy of the main component of C 1s spectra obtained for surfaces with adsorbed stannanes is 284.2 ± 0.2 eV and can be assigned to carbon atoms screened by gold substrate electrons. This value is considerably lower than that measured for the adventitious carbon impurity on gold, 284.8–285.0 eV. This difference might be accounted for by extra-atomic relaxation occurring with participation of gold electrons, which is possible for carbon atoms in the short hydrocarbon chains that are close to the gold surface. A continuous shift of C 1s binding energy with a growing length of the carbon chain has already been reported⁴⁰ for self-assembled alkanethiol layers on gold surfaces.

Adsorption of **9** from solution was studied also on Au surface sputtered by Ar⁺ ions. Surfaces cleaned in this way are known to contain considerable concentration of various defects.⁵⁷ In this experiment, the sputtered sample was taken into the open under flow of N₂ for about 10 s and immersed in a THF solution of **9**, followed by the usual rinsing with pure THF, drying in a stream of N₂, and insertion into the spectrometer with an about 15 s exposure to ambient atmosphere. This procedure produced about a monolayer of tin oxide and a low surface concentration of carbon (C/Sn = 2.2). This result demonstrates that surface defects play a significant role in adsorption and subsequent surface reactions of stannanes.

In another experiment in which a clean Au surface was exposed for 4 h to the vapor of **9** at room temperature, the C/Sn stoichiometry corresponded well to the molecular formula but the surface concentration of both carbon and tin was low, likely due to low vapor pressure of the stannane used. The presence of the component with binding energy 530.4 eV belonging to tin oxide in the spectrum of O 1s photoelectrons seems to exclude the possibility that molecules of **9** are merely molecularly adsorbed.

An attempt was made to use room-temperature scanning tunneling microscopy (STM) under ambient conditions to find the possibly present islands of tin oxide on the sample surface,

but all images looked like those of cleaned gold. It is likely that the tin oxide is not segregated into large domains but is interspersed with the alkyls on the surface.

Monolayer Blocking Properties. Information on the permeability of the monolayers was sought from an examination of cyclic voltammograms (CV) and electrochemical impedance spectra (EIS) of 2 mM [Fe(CN)₆]^{3–} in aqueous 0.1 M KNO₃ in a four-electrode electrochemical cell at a scan rate of 7 mV s^{–1}. We tested monolayers obtained after a 5-h treatment of a gold electrode with 1×10^{-4} M THF solutions of **1**, **2**, **4**, **6**, **9** and **15**. The EIS curves are shown in Figure 8. A quantitative evaluation produced the monolayer charge transfer resistance values R_{ct} listed in Table 5.

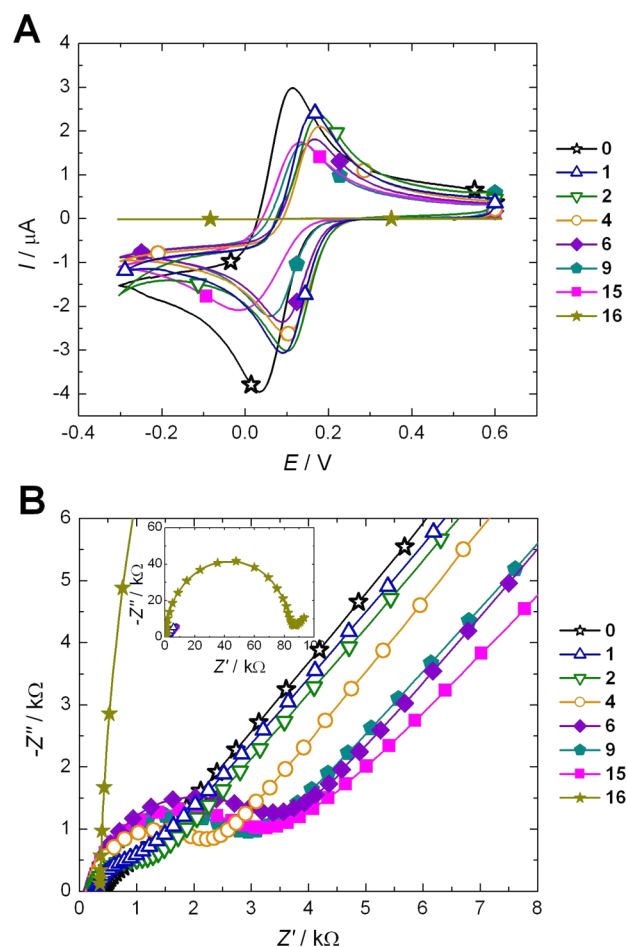


Figure 8. CV (A) and EIS (B) responses to [Fe(CN)₆]^{3–/4–} observed on the cleaned Au substrate (**0**) and monolayers produced from THF solutions of **1**, **2**, **4**, **6**, **9**, **15** and **16**.

The CV results agree with those of EIS, but the latter are a much finer tool for evaluating the access that the [Fe(CN)₆]^{3–/4–} ions have to the conducting surface, either gold or tin oxide. The results obtained after 5-h treatment of the gold electrode surface with THF solutions of **1** and **2** are nearly identical with those obtained on the cleaned gold surface, in line with the above conclusion that no insulating alkyl groups are deposited on the gold in a few hours from 1×10^{-4} M solutions in these two cases, particularly not from **1**. The slight difference with respect to the cleaned gold surface that is observed most clearly in Table 5 is attributed to the presence of a well-conducting tin oxide layer on the surface

Table 5. Charge Transfer Resistance R_{ct} of Monolayers Deposited from 1×10^{-4} M THF Solutions after 5 h^a

compd.	$R_{ct}/\text{Ohm cm}^{-2}$
0 (bare Au)	13
1	20
2	29
4	65
6	127
9	94
15	125
16	3400

^aEstimated error: $\sim \pm 5\%$.

treated with the stannane. The resistance R_{ct} of the propylated surface obtained with **4** is twice higher, and that of the butylated surface obtained with **6**, **9**, and **15** is five to six times higher. All of these values are orders of magnitude lower than the resistance of the monolayer we obtained with the long-chain thiol **16**, 3.4 kOhm cm^{-2} . The latter agrees well with the reported value of 3.6 kOhm cm^{-2} for a monolayer of decanethiol.⁵⁸

Monolayer Stability. The IR spectra of the monolayers obtained after a 4-h immersion in a 5×10^{-4} M THF solution of **2** or **5** (Figure S5) became about 10% weaker but otherwise did not change significantly after subsequent 18-h immersion in pure THF. In the case of **2**, this was tested both in THF and in chloroform, and no change was observed. However, extended immersion in a 5×10^{-4} M solution of **2** in THF caused a spectral change in the region of asymmetric CD_3 vibration. Subsequent immersion in pure THF had no further effect.

Figure 9 shows that the thermal stability of the monolayers formed from **4** and **5** is comparable to that of a monolayer formed from $n\text{-C}_{18}\text{H}_{37}\text{SH}$ (**16**), both under ambient conditions (part A) and under reduced pressure at 200 °C (part B). We have already mentioned a slight degree of removal of the monolayers during an XPS measurement in ultrahigh vacuum. In all cases, the amount of monolayer present was estimated from the integrated IR intensity in the CH or CD stretching regions.

Upon treatment with a 1×10^{-4} M solution of $\text{C}_{18}\text{H}_{37}\text{SH}$ in THF for 18 h, a film produced from a solution of **5** in THF was completely replaced with a self-assembled monolayer of the alkanethiol, as judged both by the IR spectrum (Figure S6) and an electrode blocking measurement.

DISCUSSION

Our primary goal was to establish the scope of the transfer of short n -alkyls from solutions of stannanes to a gold surface under ambient conditions, which would be convenient for practical use. This has been accomplished, primarily by examination of the IR spectra of monolayers produced from deuterated samples. Their use was also critical for establishing beyond doubt that the transferred alkyl groups attached to the surface originate in the stannane reagent and not in the solvent or in atmospheric impurities.

The IR spectra prove unequivocally that methyl groups are not transferred from the tin atom to the gold surface in THF and CHCl_3 solutions of **1** to any detectable extent even from 5×10^{-4} – 10^{-3} M solutions, nor are they transferred from 1×10^{-4} M solutions of **8**, **10**, **12**, and **14** in THF, which transfer their butyl groups to the gold surface rapidly. Since C–D stretching vibrations occur in a spectral region that is free of

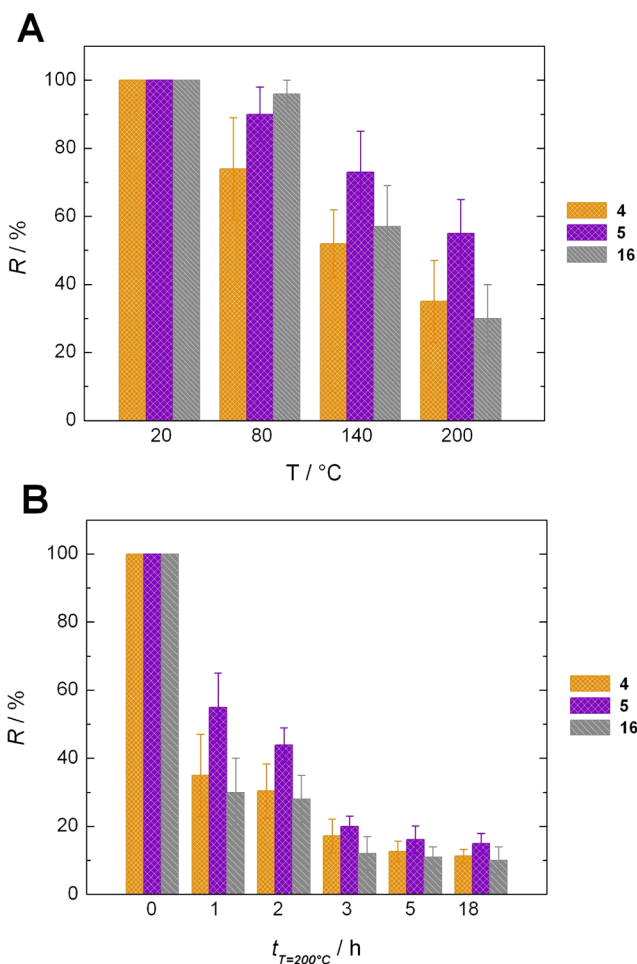


Figure 9. Thermal stability of monolayers deposited from **4** (orange), **5** (violet), and $n\text{-C}_{18}\text{H}_{37}\text{SH}$ (**16**, gray). R is the percent of monolayer remaining, evaluated from the ratio of final to initial integrated IR intensity in the 2800–3000 (**4**, **16**) or 2000–2300 (**5**) cm^{-1} region. (A) In laboratory air, 1 h at each temperature. (B) At 200 °C, under 1.5 mbar pressure.

other interferences, and since we have a comparison in the spectrum of the monolayer produced from **3**, we are confident that even a few percent of transfer would be detectable. At the same time, it is clear that at least some of the $\text{CD}_3\text{-Sn}$ bonds are broken, since XPS shows that tin oxide is deposited on the surface, but the CD_3 groups or the products of their further transformation apparently remain in the solvent.

The transfer of ethyl groups from **2** is very slow and requires the use of 5×10^{-4} M or higher concentrations before it proceeds at a useful rate. In contrast, within a few hours, n -propyl and n -butyl monolayers were formed on cleaned gold surface under ambient conditions after treatment with a 1×10^{-4} M THF solution of stannanes **3**–**15** that carry propyl or butyl groups on the tin atom. In this regard, they resemble the previously examined stannyl tosylates carrying one, two, or three n -octadecyl chains on the tin,¹³ and it is likely that stannanes carrying n -alkyls of intermediate lengths will behave similarly.

Not surprisingly, the ellipsometric thickness of the monolayers and the electrochemical charge transfer resistance increase in the order ethyl, propyl, butyl, but otherwise all the self-limited monolayers have similar properties. The contact angle and also the IR spectra, except for obvious differences due

to isotopic labeling, are essentially indistinguishable regardless of the choice of the propyl-carrying stannane **3** or **4** or any one of the butyl-carrying stannanes **5–13**. The peak positions in the IR spectra indicate that the alkyl groups are not all in the anti conformation but are disordered. Order would not be expected for alkyl groups as short as propyl or butyl, but it was not seen even for the long alkyls investigated earlier.¹³ The poor blocking of the surface that is clearly demonstrated by the electrochemical experiments could be due to a disordered and permeable nature of the alkyl monolayer itself, but in part could also reflect the conducting nature of tin oxide. We cannot state with certainty whether the relatively low coverage density is homogeneous or whether areas covered with tin oxide coexist with areas relatively densely coated with alkyl groups. The fact that we were unable to observe any tin oxide islands by STM makes the former situation more likely.

The amount of tin oxide present in the monolayer is the only property in which the monolayers obtained from different stannanes differ significantly, as it varies from 10 to 60% of a tin monolayer. The presence of tin oxide follows from the XPS lines for Sn 3d and O 1s and is compatible with the absence of C–D stretches in the IR spectra of monolayers produced from stannane precursors that carry a CD₃ group on the tin atom. The variation in tin concentration is presently difficult to interpret and suggests sensitivity to factors that are not under control, such as the exact nature of disorder on the gold surface. A possible role of defect density is also indicated by XPS results for a monolayer deposited on an ion sputtered gold surface, which show a high concentration of tin and a low C/Sn ratio (Table 4). The remainder of the elemental composition found by XPS, in particular the content of oxygen, appears to be affected by the presence of random impurities. The absence of clear signatures of the presence of oxygen in the IR spectra presumably reflects the lower sensitivity of this method, although an unfavorable orientation of the IR transition moments on the surface might also play a role.

The monolayers are stable to either solvent for many hours. Their stability toward most chemical reagents is somewhat lower than that of the more tightly packed alkanethiol monolayers and only the resistance to oxidants and to thermal desorption is a little higher. In these respects our layers again appear to be completely analogous to the previously reported monolayers formed from the covalent stannyl salts analogous to **15** but containing one to three long alkyl chains.¹³

A monolayer of unknown structure is adsorbed on the gold surface from THF alone, but not in the presence of a stannane. It does not evaporate spontaneously at room temperature, but is readily displaced upon treatment with a stannane solution. In spite of the very convincing absence of C–D stretching intensity in the IR after an attempted methyl transfer from **1**, XPS shows an increase in the amount of carbon present after treatment of the surface with **1**, and this may be an indication of imperfect removal of the layer physisorbed from THF alone.

Although more detailed investigations are clearly needed to establish the manner in which the alkyls are attached to the gold surface in the monolayers and to elucidate the mechanism by which the alkyl transfer takes place, some preliminary comments can already be provided. The only prior mechanistic investigation of the transfer of alkyl groups from the tin atom of a stannane to gold surface that we are aware of is an ultrahigh vacuum (UHV) study of benzyltrimethylstannane interacting with Au(111) and Au(110) at low temperature.¹⁹ Only the benzylic C–Sn bond was cleaved selectively, and this was

rationalized plausibly by the stability of the benzyl relative to the methyl radical. On Au(110) but not on Au(111) the radical attached to the surface through a C–Au bond. It is not clear how relevant the conclusions of the UHV study are for the mechanism that applies in solution under ambient conditions. It would certainly be difficult to rationalize the vast difference between the reactivity of a propyl and an ethyl group by an argument based on bond energy differences, and the proposed formation of trialkylstannyl groups attached to gold can be safely excluded in our case.

For the reaction in solution, it is clear that the original proposals,^{13,15} still considered viable,¹⁹ were incorrect. An intact trialkylstannyl group is not transferred to the gold surface to form an R₃Sn–Au bond. For instance, when butyls are transferred to the surface by treatment with a solution of **8**, **10**, or **12**, no C–D stretching intensity appears in the IR spectra of the monolayers. The fact that the stannanes **5–15** all deposit monolayers with identical properties except for differences in isotopic composition is best accommodated by modifying the proposal¹⁵ that the alkyl groups are transferred from the tin atom of a stannane to the gold surface with the formation of C–Au and R₃Sn–Au bonds. The formation of C–Au bonds was convincingly supported by comparison with the behavior of an alkylgold compound, and it has a close analogy in the alkylation of gold surfaces with organomercurials,^{20,21} which deposit alkyl groups along with elemental mercury.

There was no prior evidence for the proposed formation of R₃Sn–Au bonds in the gold surface alkylation process, and now there is firm evidence against it. What remains to be done is to suggest an alternate fate for the tin-containing remainder of the stannane molecule. The present XPS finding that under ambient conditions tin is present in the form of an oxide suggests that the alkyl transfer process involves an intermediate in which tin is hypovalent and susceptible to attack by oxygen. An example would be a loss of two alkyls from the tin atom in a process resembling reductive elimination, combined with an attachment of one or both of them to the gold surface. This process would generate a stannylene or, repeated twice, a tin atom. Low-valent tin would then likely undergo secondary reactions with oxygen from the atmosphere and form a tin oxide. Such a scenario would be quite analogous to what has been observed with organomercurials,^{20,21} and it is also compatible with the observation that alkylsilanes are unreactive, since silylenes are less readily formed than stannylenes. However, we cannot at present exclude the possibility that oxygen participates already in the original alkyl transfer reaction. The observation that the monolayer forming reactions did not provide any indication of strong sensitivity to the choice of solvent and in all cases tested (**1**, **2**, **3**, **12**) yielded very similar limiting thickness and IR spectra from chloroform and from THF, at comparable rates, would be compatible with a reaction mechanism that does not involve ions. The weak dependence of the rate of film formation on butylstannane structure, with only a factor of several fold between various choices of the other alkyls located on the tin atom, or even of a tosyloxy group, would be understandable, as would be the small if any effect of deuteration of the butyl or methyl groups. Also, the initial crude kinetic observations reported here for the stannane **6** demonstrate that at least in this case the rate dependence on the bulk concentration *c* is of much lower than first order, compatible with the above suggestion that more than a single butyl group may be transferred from the same tin atom to the surface.

With the limited information available presently, it would be fruitless to speculate about further details of the mechanism, or about the exact nature of the attachment of the alkyl group to the gold surface.

SUMMARY

Under ambient conditions, treatment of a gold surface with a dilute solution of an alkylstannane whose tin atom carries either one or no leaving groups, and 1–4 alkyls longer than methyl, deposits a disordered and nonblocking stable monolayer that contains the longer alkyl and a tin oxide, but does not contain the methyl or the leaving group. The previously proposed structure of the monolayer was incorrect in that it does not contain trialkylstannyl groups. It is proposed that the alkyl transfer to the gold surface involves a process similar to reductive elimination, which produces a low-valent tin species that is susceptible to oxidation by ambient oxygen. A preliminary examination of the kinetics of film formation from **6** showed that the order of the reaction with respect to the bulk stannane concentration is much less than one, and this result is most readily accommodated by postulating that more than one alkyl residue is transferred from the same tin atom. The monolayer is thermally somewhat more stable than the compact monolayers produced with alkanethiols. Considering that it is not dense, the monolayer is surprisingly stable to chemical reagents, including oxidants.

The detailed mode of attachment of the alkyl group to the gold surface atoms and the detailed mechanism of alkyl transfer to the surface remain to be investigated. The mechanism proposed to be involved in the case of benzyltrimethylstannane under UHV conditions¹⁹ does not readily account for our observations under ambient solution conditions, in particular for the difference in the behavior of ethyl and propyl groups.

EXPERIMENTAL SECTION

Monolayer Formation. The monolayers were prepared on flame-annealed gold layers on two different substrates. Since we were unable to perform ellipsometry reliably on Au/mica, and this tool was our primary means of detecting the formation of a self-limiting monolayer, we used Au/glass with a titanium bonding layer for all measurements except XPS. A gold coated glass plate (Platypus Technologies) was first cleaned in a piranha solution (3:1 sulfuric acid and hydrogen peroxide) at 90 °C, rinsed with H₂O (18.2 MΩ) followed with absolute ethanol, and dried under nitrogen. Subsequently, the substrates were flame annealed, cooled in dry THF and then immersed in a 1×10^{-4} M solution of a stannane in dry THF under ambient atmosphere in the dark for a period of time ranging from 1 min to 18 h. The plates were then removed from the solution, rinsed thoroughly with the solvent used and dried under a stream of nitrogen. XPS measurements indicated variable small amounts of TiO₂ impurity but this variation did not seem to affect the reproducibility of the results.

Since we experienced considerable difficulty in avoiding the presence of small amounts of TiO₂ in the flame annealing of these Au/glass samples, and wished to perform XPS measurements on monolayers free of this contaminant, samples for XPS were prepared on gold-coated mica (Glimmer V3, Plano GmbH). Atomically flat Au(111) surfaces were obtained by flame annealing of the substrates in a butane flame. Then the substrates were immersed in a 5×10^{-4} M solution of **1–15** under ambient atmosphere for 4 h. Although these samples were very suitable for XPS measurements, we were unable to obtain high-quality IR, ellipsometry, and electrochemical blocking results for them.

Monolayer Characterization. Variable Angle Stokes Ellipsometer (Geartner Scientific, U.S.A.), Contact Angle Goniometer (CAM 101, KSV Instruments Ltd., Finland), and Polarization Modulation Infrared

Reflection Absorption Spectrometer (PM-IRRAS, Thermo Fisher Scientific, U.S.A.) were used. All measurements of ellipsometric thickness, contact angle, and IR spectra were repeated five times for each immersion time and each stannane. The value 1.74 was adopted for the index of refraction in the evaluation of ellipsometric thickness of films that contained both alkyl groups and tin oxide, and the value 2.0 was used for films containing only tin oxide. The value 1.47 was adopted for films produced from an alkanethiol. The electrochemical blocking properties were examined using 2 mM Fe(CN)₆^{3–} in 0.1 M KNO₃ aqueous solution, a home-built four-electrode electrochemical system for CV and EIS with a Au working electrode, Pt auxiliary electrode, Ag/AgCl wire as DC reference electrode, and a high-frequency Pt electrode,²⁰ and an AutoLab PGSTAT302N potentiostat (Metrohm Autolab, The Netherlands). The procedure used for the derivation of charge transfer resistance R_{ct} values from EIS curves was described previously.⁵⁹ The STM instrument was Agilent 5500 SPM. Self-cut Pt/Ir (80:20) tips were used as a probe.

The X-ray photoelectron spectra (XPS) of the samples were measured using multitechnique spectrometers ESCA 310 (Gammadata Scienta, Sweden) and ESCA3MkII (VG Scientific, UK) both equipped with a hemispherical electron analyzer operated at constant pass energy. Al K α radiation (1486.6 eV) was used for electron excitation. The binding energy scale of the spectrometers was calibrated using the Au 4f_{7/2} (84.0 eV) and Cu 2p_{3/2} (932.6 eV) photoemission lines. The pressure of residual gases in the analysis chamber during spectra acquisition was 6×10^{-10} mbar. The typical time needed for transferring the sample from argon atmosphere via ambient air to the UHV chamber of the spectrometer was less than 3 min. The spectra were measured at room temperature and collected at a detection angle of 45° with respect to the macroscopic sample surface plane unless mentioned otherwise. Survey scan spectra and high resolution spectra of Sn 3d, C 1s, O 1s and Au 4f photoelectrons were measured. The spectra were curve fitted after subtraction of Shirley background⁶⁰ using the Gaussian–Lorentzian line shape and the damped nonlinear least-squares algorithms (software XPSPEAK 4.1).⁶¹ Quantification of elemental concentrations was accomplished by correcting integrated intensities of photoelectron peaks for the transmission function of the electron analyzer and the pertinent photoionization cross sections.⁵⁰ Surface concentration of tin was calculated from the Sn 3d and Au 4f spectra intensities assuming a layer growth and using the XPS Multiquant software.⁶²

Materials. Me₃SnCl, Me₂SnCl₂, MeSnCl₃, SnCl₄, CH₃CH₂CH₂Br, CD₃I (99.5 atom % D), Mg, and *p*-toluenesulfonic acid were purchased from Sigma-Aldrich and used without further purification. *n*-Bu₄Sn (**6**) was purchased from ABCR GmbH. CD₃CH₂CH₂Br^{63,64} and (CD₃)₃SnCl⁶⁵ were prepared according to published procedures. THF was distilled from sodium and benzophenone under argon immediately prior to use. Benzene was distilled from sodium under argon immediately prior to use.

Synthesis. All reactions were carried out under argon atmosphere with dry solvents, freshly distilled under anhydrous conditions, unless otherwise noted. Standard Schlenk and vacuum line techniques were employed for all manipulations of air- or moisture-sensitive compounds. Yields refer to isolated, chromatographically and spectroscopically homogeneous materials, unless otherwise stated. Melting points were determined with a standard apparatus and are uncorrected. ¹H and ¹³C spectra were acquired at 25 °C with 400 and 500 MHz spectrometers. ¹H and ¹³C spectra were referenced to residual solvent peaks. The content of deuterium was determined by elemental analysis as protium, since this method is not able to recognize the difference between them (both are converted to water during the analysis and its amount is finally determined by thermal conductivity; thermal conductivities of H₂O and D₂O are the same).

Tetramethylstannane-d₁₂ (1**).** *Procedure A.* A solution of iodomethane-d₃ (10.03 g, 69.2 mmol) in diethyl ether (50 mL) was added dropwise to a stirred mixture of Mg (1.81 g, 74.5 mmol) in diethyl ether (50 mL) under inert atmosphere at RT. The reaction mixture was stirred 2 h at RT and then diethyl ether was evaporated and the residue was dried under reduced pressure at 50 °C for 4 h. Dry

benzene (50 mL) was added to the residue and the resulting slurry was cooled to 0 °C. A solution of tetrachlorostannane (3.72 g, 14.0 mmol) in dry benzene (20 mL) was added dropwise to the vigorously stirred slurry and the mixture was stirred overnight at RT under argon. The reaction was quenched by slow addition of water (10 mL) at 0 °C. The mixture was extracted with water (2 × 10 mL), dried over Na₂SO₄, filtered, and purified by short column chromatography (10 g of silicagel, pentane). Pentane was distilled off and the crude product was purified by distillation (bp 74–76 °C) using a packed column to give **1** as colorless liquid (1.66 g, 8.70 mmol, 63%). ²H NMR (76.7 MHz, CH₂Cl₂) δ −0.13 (s, 12D, CD₃-Sn). ¹³C NMR (125.7 MHz, CD₂Cl₂) δ −10.19 (sep, J_{C,D} = 19.5 Hz). ¹¹⁹Sn (186.4 MHz, CD₂Cl₂) δ −1.02 (bs). IR (ATR) 2231, 2118, 922 cm^{−1}. HRMS (EI) for (C₄²H₁₂Sn⁺) calcd 192.0714, found 192.0710.

Tetra(ethyl-d₅)stannane (2). *Procedure A.* 1-Bromoethane-d₅ (5.12 g, 44.9 mmol), Mg (1.20 g, 49.4 mmol), tetrachlorostannane (2.29 g, 8.79 mmol). Yield of **2**, 1.23 g (5.94 mmol, 68%) as colorless oil, bp 62–64 °C/10 Torr. ²H NMR (76.7 MHz, CDCl₃) δ 0.75 (bs, 8D, CD₂), 1.12 (bs, 12D, CD₃). ¹³C NMR (125.7 MHz, CDCl₃) δ −1.55 (quin, J_{C,D} = 19.5 Hz, CD₂), 9.89 (sep, J_{C,D} = 19.1 Hz, CD₃). ¹¹⁹Sn NMR (186.4 MHz, CDCl₃) δ 3.14 (s). IR (ATR) 2211, 2200, 2177, 2135, 2065, 1118, 1058, 719, 693 cm^{−1}. MS-Cl, m/z (%) 256.0 (center of isotope cluster, M, 5), 222.0 (center of isotope cluster, M − C₂D₅, 100). Anal. Calcd for C₄²H₂₀Sn (207.04): C, 37.67; H, 7.92. Found: C, 37.82; H, 8.22.

Tetra(propyl-3,3,3-d₃)stannane (3). *Procedure A.* 1-Bromopropane-3,3,3-d₃ (2.01 g, 16.7 mmol), Mg (0.43 g, 17.7 mmol), tetrachlorostannane (1.06 g, 4.00 mmol). Yield of **3**, 918 mg (3.0 mmol, 76%) as colorless oil, bp 103–106 °C/10 Torr. ¹H NMR (500 MHz, CDCl₃) δ 0.82 (m, 8H, CD₃−CH₂−CH₂−Sn), 1.52 (m, 8H, CD₃−CH₂−CH₂−Sn). ²H NMR (76.7 MHz, CDCl₃) δ 0.92 (m, 12D, CD₃−CH₂−CH₂−Sn). ¹³C NMR (126 MHz, CDCl₃) δ 11.73 (s, CD₃−CH₂−CH₂−Sn), 18.07 (sep, J_{C,D} = 19.0 Hz, CD₃−CH₂−CH₂−Sn), 20.19 (s, CD₃−CH₂−CH₂−Sn). ¹¹⁹Sn (186 MHz, CDCl₃) δ −16.33 (s). IR (KBr) 2923, 2901, 2856, 2816, 2226, 2209, 2138, 2122, 2110, 2088, 2070, 1459, 1420, 1331, 1321, 1260, 1168, 1150, 1112, 1054, 1026, 963, 933, 923, 904, 694, 647, 502 cm^{−1}. MS-Cl, m/z (%) 304.2 (center of isotope cluster, M, 5), 258.1 (center of isotope cluster, M − CH₂−CH₂−CD₃, 100). HRMS (CI) for (C₁₂¹H₁₆²H₁₂Sn⁺) calcd 304.1966, found 304.1973. Anal. Calcd for C₁₂¹H₁₆²H₁₂Sn (303.14): C, 47.55; H, 9.70. Found: C, 47.58; H, 9.42.

Tetrapropylstannane (4). *Procedure A.* 1-Bromopropane (7.32 g, 53.4 mmol), Mg (1.23 g, 50.6 mmol), tetrachlorostannane (3.14 g, 11.8 mmol). Yield of **4**, 3.24 g (11.1 mmol, 95%), bp 112–114 °C/10 Torr. The ¹H NMR, ¹³C NMR and MS spectra were consistent with published data.^{66,67} ¹¹⁹Sn NMR (186 MHz, CDCl₃) δ −16.56 (s). IR (ATR) 2952, 2923, 2898, 2886, 1454, 1417, 1339, 1276, 694, 662 cm^{−1}. Anal. Calcd for C₁₂H₂₈Sn (291.06): C, 49.52; H, 9.70. Found: C, 49.25; H, 9.50.

Tetra(n-butyl-d₉)stannane (5). *Procedure A.* 1-Bromobutane-d₉ (5.10 g, 34.9 mmol), Mg (0.84 g, 34.6 mmol), tetrachlorostannane (1.82 g, 6.8 mmol). Yield of **5**, 1.66 g (4.8 mmol, 70%) as colorless oil, bp 148–150 °C/10 Torr. ²H NMR (76.7 MHz, CDCl₃) δ 0.77 (bs, 8D, CD₃−CD₂−CD₂−CD₂−Sn), 0.84 (bs, 12D, CD₃−CD₂−CD₂−CD₂−Sn), 1.24 (bs, 8D, CD₃−CD₂−CD₂−CD₂−Sn), 1.41 (bs, 8D, CD₃−CD₂−CD₂−CD₂−Sn). ¹³C NMR (125.7 MHz, CDCl₃) δ 7.48 (quin, J_{C,D} = 19.6 Hz, CD₃−CD₂−CD₂−CD₂−Sn), 12.57 (sep, J_{C,D} = 18.9 Hz, CD₃−CD₂−CD₂−CD₂−Sn), 26.04 (quin, J_{C,D} = 18.9 Hz, CD₃−CD₂−CD₂−CD₂−Sn), 27.96 (quin, J_{C,D} = 19.0 Hz, CD₃−CD₂−CD₂−CD₂−Sn). ¹¹⁹Sn NMR (186.4 MHz, CDCl₃) δ −12.13 (s). IR (ATR) 2214, 2198, 2102, 2070, 1157, 1085, 1058, 1029 cm^{−1}. MS-Cl, m/z (%) 318.3 (center of isotope cluster, M − C₄D₉, 100), 252.2 [center of isotope cluster, M − 2(C₄D₉), 10]. Anal. Calcd for C₁₆²H₃₆Sn (347.17): C, 50.12; H, 9.46. Found: C, 50.14; H, 9.44.

Tri-n-butylmethylstannane (7). *Procedure B.* A solution of methylmagnesium bromide in diethyl ether (3.0 M, 4.60 mL, 13.8 mmol) was added dropwise to a stirred solution of tributylstannyl chloride (3.24 g, 9.9 mmol) in diethyl ether (80 mL) under inert atmosphere at 0 °C. The reaction mixture was stirred 2 h at RT and then quenched with water (2 mL). Diethyl ether was evaporated on

vacuum evaporator and CH₂Cl₂ (80 mL) was added to the residue. The mixture was extracted with water (2 × 10 mL), dried over Na₂SO₄, filtered and evaporated on vacuum evaporator. The crude product was distilled under vacuum (103–105 °C/6.0 Torr) to give 2.78 g (9.1 mmol) of **7** (yield, 91%) as colorless oil. The ¹H NMR, ¹³C NMR and MS spectra were consistent with the data published in literature.⁶⁸ ¹¹⁹Sn (186 MHz, CDCl₃) δ −4.77 (s). IR (ATR) 2985, 2922, 2872, 2845, 1464, 1457, 1418, 1376, 1189, 727 cm^{−1}. Anal. Calcd for C₁₃H₃₀Sn (305.08): C, 51.18; H, 9.91. Found: C, 51.06; H, 9.94.

Tri-n-butyl(methyl-d₃)stannane (8). *Procedure B.* Methyl-d₃-magnesium iodide in diethyl ether (1.0 M, 18.0 mL, 18.0 mmol), tributylstannyl chloride (4.19 g, 12.9 mmol). Yield of **8**, 3.77 g (12.2 mmol, 95%) as colorless oil, bp 103–105 °C/6.0 Torr. ¹H NMR (400 MHz, CDCl₃) δ 0.81 (m, 6H, CH₃−CH₂−CH₂−CH₂−Sn), 0.89 (t, J = 7.27 Hz, 9H, CH₃−CH₂−CH₂−CH₂−Sn), 1.30 (m, 6H, CH₂), 1.46 (m, 6H, CH₂). ¹³C NMR (125.7 MHz, CDCl₃) δ 9.42 (s, CH₃−CH₂−CH₂−CH₂−Sn), 13.71 (s, CH₃−CH₂−CH₂−CH₂−Sn), 27.26 (s, CH₂), 29.18 (s, CH₂). ²H NMR (76.7 MHz, CH₂Cl₂) δ −0.64 (m, 3D, CD₃-Sn). ¹¹⁹Sn (186.4 MHz, CH₂Cl₂) δ −5.99 (s). IR (ATR) 2956, 2922, 2872, 2848, 2229, 2110, 1464, 1458, 1418, 1376, 918, 873, 691, 663 cm^{−1}. MS-Cl, m/z (%) 309.2 (center of isotope cluster, M, 1), 289.1 (center of isotope cluster, M − CD₃, 30), 250.1 (center of isotope cluster, M − C₄H₉, 100). Anal. Calcd for C₁₃¹H₂₇²H₃Sn (308.11): C, 50.68; H, 9.81. Found: C, 50.39; H, 9.77.

Di-n-butylidimethylstannane (9). *Procedure C.* A solution of methylmagnesium bromide in diethyl ether (3.0 M, 10.3 mL, 31.0 mmol) was added dropwise to a stirred solution of dibutylstannyl dichloride (3.14 g, 10.3 mmol) in diethyl ether (50 mL) under inert atmosphere at 0 °C. The reaction mixture was stirred 2 h at RT and then quenched with water (1 mL). Diethyl ether was evaporated on vacuum evaporator and CH₂Cl₂ (50 mL) was added to the residue. The mixture was extracted with water (2 × 10 mL), dried over Na₂SO₄, filtered and evaporated on vacuum evaporator. The crude product was distilled under vacuum (90–92 °C/6.0 Torr) to give 2.56 g (9.7 mmol) of **9** (yield, 94%) as colorless oil. ¹H NMR, ¹³C NMR and MS spectra were consistent with published data.⁶⁸ ¹¹⁹Sn (186 MHz, CDCl₃) δ −1.19 (s). IR (ATR) 2952, 2923, 2896, 2854, 2848, 1464, 1458, 1418, 1377, 1187, 873, 863, 749, 738 cm^{−1}. Anal. Calcd for C₁₀H₂₄Sn (263.01): C, 45.67; H, 9.20. Found: C, 45.97; H, 9.13.

Di-n-butylidimethyl-d₃stannane (10). *Procedure C.* Methyl-d₃-magnesium iodide in diethyl ether (1.0 M, 14.2 mL, 14.2 mmol), dibutylstannyl dichloride (1.49 g, 4.9 mmol). Yield of **10**, 1.15 g (4.3 mmol, 86%) as colorless oil, bp 90–92 °C/6.0 Torr. ¹H NMR (400 MHz, CDCl₃) δ 0.81 (t, ³J_{H,H} = 8.0 Hz, 4H, CH₃−CH₂−CH₂−CH₂−Sn), 0.89 (t, ³J_{H,H} = 8.0 Hz, 6H, CH₃−CH₂−CH₂−CH₂−Sn), 1.29 (m, 4H, CH₂), 1.46 (m, 4H, CH₂). ²H NMR (76.7 MHz, CH₂Cl₂) δ −0.19 (m, 6D, CD₃-Sn). ¹³C APT (126 MHz, CDCl₃) δ 10.01 (s, CH₃−CH₂−CH₂−CH₂−Sn), 13.70 (s, CH₃−CH₂−CH₂−CH₂−Sn), 27.10 (s, CH₂), 29.06 (s, CH₂). Signals of deuterated methyls overlapped by noise. ¹¹⁹Sn (186.4 MHz, CH₂Cl₂) δ −2.57 (s). IR (KBr) 2956, 2923, 2898, 2874, 2846, 2229, 2116, 1464, 1419, 919 cm^{−1}. MS, m/z (%) 252.1 (center of isotope cluster, M − CD₃, 75), 213.1 (center of isotope cluster, M − C₄H₉, 100). Anal. Calcd for C₁₀¹H₁₈²H₆Sn (269.05): C, 44.64; H, 8.99. Found: C, 44.65; H, 9.00.

n-Butyltrimethylstannane (11). *Procedure D.* Magnesium (470 mg, 19.3 mmol) was placed to a three necked flask equipped with Dimroth condenser and dry diethyl ether (60 mL) was added. A solution of 1-bromobutane (2.43 g, 17.7 mmol) in diethyl ether (10 mL) was added dropwise at RT and the resulting mixture was stirred 2 h at the same temperature. The reaction mixture was cooled to 0 °C and a solution of trimethylstannyl chloride (3.21 g, 16.1 mmol) in diethyl ether (10 mL) was added dropwise. The reaction mixture was stirred 4 h at RT and then quenched with water (5 mL). Diethyl ether was evaporated on vacuum evaporator and CH₂Cl₂ (80 mL) was added to the residue. The mixture was extracted with water (2 × 30 mL), dried over Na₂SO₄, filtered and evaporated on vacuum evaporator. The residue was purified by short column chromatography (10 g of silicagel, pentane) and the crude product was distilled (152–154 °C) to give 3.26 g (14.7 mmol) of **11** (yield, 92%) as colorless

liquid. ^1H NMR, ^{13}C NMR and MS spectra were consistent with the data published in literature.⁶⁸ ^{119}Sn (186 MHz, CDCl_3) δ 0.46 (s). IR (ATR) 2958, 2922, 2873, 2846, 1464, 1458, 1419, 1377, 1293, 1251, 1188, 1071, 873, 761, 668 cm^{-1} . Anal. Calcd for $\text{C}_7\text{H}_{18}\text{Sn}$ (220.93): C, 38.06; H, 8.21. Found: C, 37.80; H, 8.21.

***n*-Butyltri(methyl- d_3)stannane (12).** A solution of methyl- d_3 -magnesium iodide in diethyl ether (1.0 M, 50.1 mL, 13.8 mmol) was added dropwise to a stirred solution of *n*-butylstannyl chloride (3.53 g, 12.5 mmol) in diethyl ether (50 mL) under inert atmosphere at 0 °C. The reaction mixture was stirred 2 h at RT and then quenched with water (5 mL). Diethyl ether was evaporated on vacuum evaporator and CH_2Cl_2 (80 mL) was added to the residue. The mixture was extracted with water (2 \times 20 mL), dried over Na_2SO_4 , filtered and evaporated on vacuum evaporator. The crude product was distilled (152–154 °C) to give 1.80 g (7.8 mmol) of **12** (yield, 63%) as colorless liquid. ^1H NMR (400 MHz, CDCl_3) δ 0.82 (m, 2H, $\text{CH}_3\text{--CH}_2\text{--CH}_2\text{--CH}_2\text{--Sn}$), 0.89 (t, J = 7.27 Hz, 3H, $\text{CH}_3\text{--CH}_2\text{--CH}_2\text{--CH}_2\text{--Sn}$), 1.30 (m, 2H, CH_2), 1.48 (m, 2H, CH_2). ^{13}C NMR (100 MHz, CDCl_3) δ 10.76 (s, $\text{CH}_3\text{--CH}_2\text{--CH}_2\text{--CH}_2\text{--Sn}$), 13.85 (s, $\text{CH}_3\text{--CH}_2\text{--CH}_2\text{--CH}_2\text{--Sn}$), 27.14 (s, CH_2), 29.13 (s, CH_2). ^2H NMR (76.7 MHz, CH_2Cl_2) δ -0.16 (m, 12D, $\text{CD}_3\text{--Sn}$). ^{119}Sn (186.4 MHz, CH_2Cl_2) δ -1.45 (s). IR (ATR) 2956, 2872, 2896, 2229, 2116, 1464, 1457, 1412, 1377, 1292, 1250, 1151, 919, 873, 661 cm^{-1} . MS, m/z (%) 229.1 (center of isotope cluster, M, S), 211.0 (center of isotope cluster, M - CD_3 , 100), 172.0 (center of isotope cluster, M - C_4H_9 , 50). Anal. Calcd for $\text{C}_7^1\text{H}_9^2\text{H}_9\text{Sn}$ (229.98): C, 36.56; H, 7.86. Found: C, 36.56; H, 8.00.

***n*-Butyl- d_9 -trimethylstannane (13).** Procedure D. 1-Bromobutane- d_9 (2.54 g, 17.4 mmol), magnesium (460 mg, 18.9 mmol), trimethylstannyl chloride (3.07 g, 15.4 mmol). Yield of **13**, 3.23 g (14.0 mmol, 76%), bp 150–152 °C. ^1H NMR (500.0 MHz, CDCl_3) δ 0.03 (s, 9H, $\text{CH}_3\text{--Sn}$). ^2H NMR (76.7 MHz, CDCl_3) δ 0.80 (bs, 2D, $\text{CD}_3\text{--CD}_2\text{--CD}_2\text{--CD}_2\text{--Sn}$), 0.84 (bs, 3D, $\text{CD}_3\text{--CD}_2\text{--CD}_2\text{--CD}_2\text{--Sn}$), 1.24 (bs, 2D, $\text{CD}_3\text{--CD}_2\text{--CD}_2\text{--CD}_2\text{--Sn}$), 1.43 (bs, 2D, $\text{CD}_3\text{--CD}_2\text{--CD}_2\text{--CD}_2\text{--Sn}$). ^{13}C NMR (125.7 MHz, CDCl_3) δ -10.41 (s, $\text{CH}_3\text{--Sn}$), 9.78 (quin, $J_{\text{C,D}}$ = 19.1 Hz, $\text{CD}_3\text{--CD}_2\text{--CD}_2\text{--CD}_2\text{--Sn}$), 12.54 (sep, $J_{\text{C,D}}$ = 19.1 Hz, $\text{CD}_3\text{--CD}_2\text{--CD}_2\text{--CD}_2\text{--Sn}$), 25.60 (quin, $J_{\text{C,D}}$ = 19.1 Hz, $\text{CD}_3\text{--CD}_2\text{--CD}_2\text{--CD}_2\text{--Sn}$), 27.59 (quin, $J_{\text{C,D}}$ = 19.1 Hz, $\text{CD}_3\text{--CD}_2\text{--CD}_2\text{--CD}_2\text{--Sn}$). ^{119}Sn NMR (186.4 MHz, CDCl_3) δ 0.28 (s). HRMS, (EI) for ($\text{C}_7^1\text{H}_9^2\text{H}_9\text{Sn}^+$) calcd 231.0995, found 231.1005. IR (ATR) 2977, 2913, 2215, 2210, 2102, 2089, 2069, 1189, 1058, 769 cm^{-1} . Anal. Calcd for $\text{C}_7^1\text{H}_9^2\text{H}_9\text{Sn}$ (229.98): C, 36.56; H, 7.90. Found: C, 36.17; H, 8.00.

***n*-Butyl- d_9 -tri(methyl- d_3)-stannane (14).** Procedure D. 1-Bromobutane- d_9 (1.84 g, 12.6 mmol), magnesium (360 mg, 14.8 mmol), tri(methyl- d_3)stannyl chloride (2.21 g, 10.6 mmol). Yield of **14**, 1.84 g (7.7 mmol, 73%), bp 150–152 °C. ^2H NMR (76.7 MHz, CDCl_3) δ 0.02 (bs, 9D, $\text{CD}_3\text{--Sn}$), 0.80 (bs, 2D, $\text{CD}_3\text{--CD}_2\text{--CD}_2\text{--CD}_2\text{--Sn}$), 0.85 (bs, 3D, $\text{CD}_3\text{--CD}_2\text{--CD}_2\text{--CD}_2\text{--Sn}$), 1.24 (bs, 2D, $\text{CD}_3\text{--CD}_2\text{--CD}_2\text{--CD}_2\text{--Sn}$), 1.43 (bs, 2D, $\text{CD}_3\text{--CD}_2\text{--CD}_2\text{--CD}_2\text{--Sn}$). ^{13}C NMR (125.7 MHz, CDCl_3) δ -11.34 (sep, $J_{\text{C,D}}$ = 19.5 Hz, $\text{CD}_3\text{--Sn}$), 9.55 (quin, $J_{\text{C,D}}$ = 19.3 Hz, $\text{CD}_3\text{--CD}_2\text{--CD}_2\text{--CD}_2\text{--Sn}$), 12.55 (sep, $J_{\text{C,D}}$ = 19.0 Hz, $\text{CD}_3\text{--CD}_2\text{--CD}_2\text{--CD}_2\text{--Sn}$), 25.61 (quin, $J_{\text{C,D}}$ = 19.1 Hz, $\text{CD}_3\text{--CD}_2\text{--CD}_2\text{--CD}_2\text{--Sn}$), 27.63 (quin, $J_{\text{C,D}}$ = 19.0 Hz, $\text{CD}_3\text{--CD}_2\text{--CD}_2\text{--CD}_2\text{--Sn}$). ^{119}Sn NMR (186.4 MHz, CDCl_3) δ -1.75 (s). MS, m/z (%) 238.1 (center of isotope cluster, M, 1), 220.1 (center of isotope cluster, M - CD_3 , 100), 172.0 (center of isotope cluster, M - C_4D_9 , 30). IR (ATR) 2215, 2174, 2117, 2102, 2089, 1058, 920 cm^{-1} . Anal. Calcd for $\text{C}_7^2\text{H}_{18}\text{Sn}$ (239.04): C, 35.17; H, 7.58. Found: C, 35.37; H, 7.48.

Di-*n*-butylmethylstannyl *p*-toluenesulfonate hemihydrate (15). To a solution of stannane **9** (2.88 g, 11.0 mmol) in CH_2Cl_2 (30 mL) was added 1.89 g (11.0 mmol) *p*-toluenesulfonic acid. The resulting mixture was refluxed for 3 days. The solvent was evaporated and the residue was 15 times recrystallized from ethyl acetate to get 1.61 g (35%) of **15** as a colorless wax. ^1H NMR (500 MHz, CDCl_3) δ 0.50 (s, 3H, $\text{CH}_3\text{--Sn}$), 0.78 (t, J = 7.32 Hz, 6H, $\text{CH}_3\text{--CH}_2\text{--CH}_2\text{--CH}_2\text{--Sn}$), 1.22–1.15 (m, 8H, CH_2), 1.47 (m, 4H, $\text{CH}_3\text{--CH}_2\text{--CH}_2\text{--CH}_2\text{--Sn}$), 2.37 (s, 3H, Ar- CH_3), 7.19 (d, J = 8.2 Hz, 2H, Ar-H), 7.55 (d, J = 8.2 Hz, 2H, Ar-H). ^{13}C APT (125.7 MHz, CDCl_3) δ 0.29

(s, CH_3), 13.73 (s, CH_3), 20.93 (s, CH_2), 21.52 (s, CH_3), 26.87 (s, CH_2), 27.62 (s, CH_3), 126.04 (s, CH), 129.22 (s, CH), 139.51 (s, arom. C), 142.07 (s, arom. C). ^{119}Sn NMR (186.4 MHz, CDCl_3) δ 86.16 (s). IR (KBr) 3028, 2955, 2922, 2871, 2855, 1463, 1417, 1377, 1261, 1105, 1030, 679 cm^{-1} . HRMS, (MALDI) for ($\text{C}_{15}\text{H}_{28}\text{O}_3\text{SSn} + ^6\text{Li}^+$) calcd 415.0936, found 415.0923. Anal. Calcd for $\text{C}_{32}\text{H}_{58}\text{O}_7\text{S}_2\text{Sn}_2$ (856.35): C, 44.88; H, 6.83. Found: C, 44.87; H, 6.71.

■ ASSOCIATED CONTENT

Supporting Information

The Supporting Information is available free of charge on the ACS Publications website at DOI: 10.1021/jacs.5b07672.

Kinetic data for monolayer formation, PM-IRRAS and XPS of monolayers, NMR spectra of alkylstannanes. (PDF)

■ AUTHOR INFORMATION

Corresponding Author

*michl@eefus.colorado.edu

Notes

The authors declare no competing financial interest.

■ ACKNOWLEDGMENTS

We thank the European Research Council under the European Community's Seventh Framework Programme (FP7/2007-2013)/ERC grant agreement no. 227756, the grant agency of the Czech Republic (14-02337S), and the Institute of Organic Chemistry and Biochemistry (RVO: 61388963) and the J. Heyrovský Institute of Physical Chemistry (project no. 994115) of the Academy of Sciences of the Czech Republic. Work in Boulder was supported by the US National Science Foundation (CHE-1265922). We are grateful to Dr. Magda Hromadová for assistance with STM measurements, and to Dr. Florian von Wrochem for a useful discussion.

■ REFERENCES

- (1) Blackman, L. C. F.; Dewar, M. J. S. *J. Chem. Soc.* **1957**, 162.
- (2) Blackman, L. C. F.; Dewar, M. J. S. *J. Chem. Soc.* **1957**, 165.
- (3) Blackman, L. C. F.; Dewar, M. J. S. *J. Chem. Soc.* **1957**, 169.
- (4) Blackman, L. C. F.; Dewar, M. J. S. *J. Chem. Soc.* **1957**, 171.
- (5) Ulman, A. *Chem. Rev.* **1996**, 96, 1533.
- (6) Schreiber, F. *Prog. Surf. Sci.* **2000**, 65, 151.
- (7) Love, J. C.; Estroff, L. A.; Kriebel, J. K.; Nuzzo, R. G.; Whitesides, G. M. *Chem. Rev.* **2005**, 105, 1103.
- (8) Schoenfish, M. H.; Pemberton, J. E. *J. Am. Chem. Soc.* **1998**, 120, 4502.
- (9) Celestin, M.; Krishnan, S.; Bhansali, S.; Stefanakos, E.; Goswami, D. Y. *Nano Res.* **2014**, 7, 589.
- (10) Willey, T. M.; Vance, A. L.; Van Buuren, T.; Bostedt, C.; Terminello, L. J.; Fadley, C. S. *Surf. Sci.* **2005**, 576, 188.
- (11) Widrig, C. A.; Chung, C.; Porter, M. D. *J. Electroanal. Chem. Interfacial Electrochem.* **1991**, 310, 335.
- (12) Munakata, H.; Oyamatsu, D.; Kuwabata, S. *Langmuir* **2004**, 20, 10123.
- (13) Khobragade, D.; Stensrud, E. S.; Mucha, M.; Smith, J. R.; Pohl, R.; Stibor, I.; Michl, J. *Langmuir* **2010**, 26, 8483.
- (14) Michl, J.; Stibor, I. CZ Patent No. 302441B6, April 8, 2011.
- (15) Cheng, Z. L.; Skouta, R.; Vázquez, H.; Widawsky, J. R.; Schneebeli, S.; Chen, W.; Hybertsen, M. S.; Breslow, R.; Venkataraman, L. *Nat. Nanotechnol.* **2011**, 6, 353.
- (16) Chen, W.; Widawsky, J. R.; Vázquez, H.; Schneebeli, S. T.; Hybertsen, M. S.; Breslow, R.; Venkataraman, L. *J. Am. Chem. Soc.* **2011**, 133, 17160.
- (17) Aradhya, S. V.; Venkataraman, L. *Nat. Nanotechnol.* **2013**, 8, 399.

- (18) Widawsky, J. R.; Chen, W.; Vázquez, H.; Kim, T.; Breslow, R.; Hybertsen, M. S.; Venkataraman, L. *Nano Lett.* **2013**, *13*, 2889.
- (19) Batra, A.; Kladnik, G.; Gorjizadeh, N.; Meisner, J.; Steigerwald, M.; Nuckolls, C.; Quek, S. Y.; Cvetko, D.; Morgante, A.; Venkataraman, L. *J. Am. Chem. Soc.* **2014**, *136*, 12556.
- (20) Mucha, M.; Kaletová, E.; Kohutová, A.; Scholz, F.; Stensrud, E. S.; Stibor, I.; Pospíšil, L.; von Wrochem, F.; Michl, J. *J. Am. Chem. Soc.* **2013**, *135*, 5669.
- (21) Scholz, F.; Kaletová, E.; Stensrud, E. S.; Ford, W. E.; Kohutová, A.; Mucha, M.; Stibor, I.; Michl, J.; von Wrochem, F. *J. Phys. Chem. Lett.* **2013**, *4*, 2624.
- (22) Zheng, X.; Mulcahy, M. E.; Horinek, D.; Galeotti, F.; Magnera, T. F.; Michl, J. *J. Am. Chem. Soc.* **2004**, *126*, 4540.
- (23) Mulcahy, M. E.; Magnera, T. F.; Michl, J. *J. Phys. Chem. C* **2009**, *113*, 20698.
- (24) Mulcahy, M. E.; Bastl, Z.; Stensrud, K. F.; Magnera, T. F.; Michl, J. *J. Phys. Chem. C* **2010**, *114*, 14050.
- (25) Lee, T. R.; Whitesides, G. M. *Acc. Chem. Res.* **1992**, *25*, 266.
- (26) Gooding, J. J.; Ciampi, S. *Chem. Soc. Rev.* **2011**, *40*, 2704.
- (27) Laurentius, L.; Stoyanov, S. R.; Gusarov, S.; Kovalenko, A.; Du, R.; Lopinski, G. P.; McDermott, M. T. *ACS Nano* **2011**, *5*, 4219.
- (28) McDonagh, A. M.; Zareie, H. M.; Ford, M. J.; Barton, C. S.; Ginic-Markovic, M.; Matisons, J. G. *J. Am. Chem. Soc.* **2007**, *129*, 3533.
- (29) Hong, W.; Li, H.; Liu, S.; Fu, Y.; Li, J.; Kaliginedi, V.; Decurtins, S.; Wandlowski, T. *J. Am. Chem. Soc.* **2012**, *134*, 19425.
- (30) Zhang, S.; Chandra, K. L.; Gorman, C. B. *J. Am. Chem. Soc.* **2007**, *129*, 4876.
- (31) Crudden, C. M.; Horton, J. H.; Ebralidze, I. I.; Zenkina, O. V.; McLean, A. B.; Drevniok, B.; She, Z.; Kraatz, H. B.; Mosey, N. J.; Seki, T.; Keske, E. C.; Leake, J. D.; Rousina-Webb, A.; Wu, G. *Nat. Chem.* **2014**, *6*, 409.
- (32) Leary, E.; González, M. T.; van der Pol, C.; Bryce, M. R.; Filippone, S.; Martín, N.; Rubio-Bollinger, G.; Agrait, N. *Nano Lett.* **2011**, *11*, 2236.
- (33) Evangeli, Ch.; Gillemot, K.; Leary, E.; González, M. T.; Rubio-Bollinger, G.; Lambert, C. J.; Agrait, N. *Nano Lett.* **2013**, *13*, 2141.
- (34) Kiguchi, M.; Tal, O.; Wohlthat, S.; Pauly, F.; Krieger, M.; Djukic, D.; Cuevas, J. C.; van Ruitenbeek, J. M. *Phys. Rev. Lett.* **2008**, *101*, 046801.
- (35) Kaletová, E.; Kohutová, A.; Hajduch, J.; Bastl, Z.; Michl, J. Book of Abstracts, XIV European Symposium on Organic Reactivity, September 1–6, 2013, Prague, Czech Republic, P-49.
- (36) Meals, R. N. *J. Org. Chem.* **1944**, *9*, 211.
- (37) Patnaik, P. *Handbook of Inorganic Chemicals*; McGraw-Hill: New York, 2002.
- (38) Rouhana, L. L.; Moussallem, M. D.; Schlenoff, J. B. *J. Am. Chem. Soc.* **2011**, *133*, 16080.
- (39) Hibbert, D. B.; Gooding, J. J.; Erokhin, P. *Langmuir* **2002**, *18*, 1770.
- (40) Biebuyck, H. A.; Bain, C. D.; Whitesides, G. M. *Langmuir* **1994**, *10*, 1825.
- (41) Camillone, N., III *Langmuir* **2004**, *20*, 1199.
- (42) Karpovich, D. S.; Blanchard, G. J. *Langmuir* **1994**, *10*, 3315.
- (43) Peterlinz, K. A.; Georgiadis, R. *Langmuir* **1996**, *12*, 4731.
- (44) Yang, C. S.-C.; Richter, L. J.; Stephenson, J. C.; Briggman, K. A. *Langmuir* **2002**, *18*, 7549.
- (45) Dannenberger, O.; Buck, M.; Grunze, M. *J. Phys. Chem. B* **1999**, *103*, 2202.
- (46) Jones, R. N. *Spectrochim. Acta* **1957**, *9*, 235.
- (47) Colthup, N. B.; Daly, L. H.; Wiberley, S. E. *Introduction to Infrared and Raman Spectroscopy*, 3rd ed.; Academic Press: Waltham, MA, 1990.
- (48) Bellamy, L. J. *The Infrared Spectra of Complex Molecules*, 3rd ed.; Chapman Hall: New York, 1975; Vol. 1.
- (49) Durig, J. R.; Pan, C.; Guirgis, G. A. *Spectrochim. Acta, Part A* **2003**, *59*, 979.
- (50) Scofield, J. H. *J. Electron Spectrosc. Relat. Phenom.* **1976**, *8*, 129.
- (51) Dupin, J.-C.; Gonbeau, D.; Vinatier, P.; Levasseur, A. *Phys. Chem. Chem. Phys.* **2000**, *2*, 1319.
- (52) Jiménez, V. M.; Espinós, J. P.; González-Elipe, A. R. *Surf. Sci.* **1996**, *366*, 556.
- (53) Batzill, M.; Diebold, U. *Prog. Surf. Sci.* **2005**, *76*, 47.
- (54) Akgul, F. A.; Gumus, C.; Er, A. O.; Farha, A. H.; Akhul, G.; Ufuktepe, Y.; Liu, Z. *J. Alloys Compd.* **2013**, *579*, 50.
- (55) Themlin, J.-M.; Chtaib, M.; Henrard, L.; Lambin, P.; Darville, J.; Gilles, J.-M. *Phys. Rev. B: Condens. Matter Mater. Phys.* **1992**, *46*, 2460.
- (56) Behra, P.; Lecarne-Théobald, É.; Bueno, M.; Ehrhardt, J.-J. *J. Colloid Interface Sci.* **2003**, *263*, 4.
- (57) Vishniakov, V.; Carter, G.; Donnelly, S. E. In *Ion Beam Modification of Materials*; Williams, J. S., Elliman, R. G., Ridgway, M. C., Eds.; Elsevier Sci.: Amsterdam, 1996; pp 972–977.
- (58) Janek, R. P.; Fawcett, W. R.; Ulman, A. *Langmuir* **1998**, *14*, 3011.
- (59) De Levie, R.; Pospíšil, L. *J. Electroanal. Chem. Interfacial Electrochem.* **1969**, *22*, 277.
- (60) Shirley, D. A. *Phys. Rev. B* **1972**, *5*, 4709.
- (61) A freeware program: Kwok, R. W. M. XSPEAK 4.1; Dept. of Chemistry, University of Hong Kong; Shatin, Hong Kong; <http://www.uksaf.org/xpspeak41.zip>.
- (62) Mohai, M. *Surf. Interface Anal.* **2004**, *36*, 828.
- (63) Allevi, P.; Longo, A.; Anastasia, M. *J. Labelled Compd. Radiopharm.* **1999**, *42*, 1085.
- (64) Mormann, M.; Kuck, D. *J. Mass Spectrom.* **1999**, *34*, 384.
- (65) Cuthbertson, M. J.; Wells, P. R. *J. Organomet. Chem.* **1981**, *216*, 331.
- (66) Mitchell, W. J. *Organomet. Chem.* **1976**, *121*, 177.
- (67) Gielen, M. *J. Organomet. Chem.* **1968**, *12*, 363.
- (68) Marr, I. L.; Rosales, D.; Wardell, J. L. *J. Organomet. Chem.* **1988**, *349*, 65.